Meta-learners' learning dynamics are unlike learners'

Neil C. Rabinowitz[*]

May 7, 2019
DeepMind
`ncr@google.com`

Abstract

Meta-learning is a tool that allows us to build sample-efficient learning systems. Here we show that, once meta-trained, LSTM Meta-Learners aren't just *faster* learners than their sample-inefficient deep learning (DL) and reinforcement learning (RL) brethren, but that they actually pursue fundamentally different *learning trajectories*. We study their learning dynamics on three sets of structured tasks for which the corresponding learning dynamics of DL and RL systems have been previously described: linear regression (Saxe et al., 2013), nonlinear regression (Rahaman et al., 2018; Xu et al., 2018), and contextual bandits (Schaul et al., 2019). In each case, while sample-inefficient DL and RL Learners uncover the task structure in a staggered manner, meta-trained LSTM Meta-Learners uncover almost all task structure concurrently, congruent with the patterns expected from Bayes-optimal inference algorithms. This has implications for research areas wherever the learning behaviour itself is of interest, such as safety, curriculum design, and human-in-the-loop machine learning.

1. Introduction

It is widely recognized that the major paradigm of deep learning is sample inefficient. At the same time, many real-world tasks that an intelligent system needs to perform require learning at much faster time-scales, leveraging the data from only a few examples. Yet moving from sample-inefficient learning to sample-efficient learning may not be simply a matter of speeding things up.

Here we investigate one potential point of difference between sample-inefficient learners and sample-efficient ones: the *order* in which they pick up structure in learning problems.

We explore this through a series of studies on pairs of learning systems drawn from related but different paradigms: Deep Learning and Reinforcement Learning on the one hand, and (memory-based) meta-learning (Schmidhuber et al., 1996; Thrun and Pratt, 1998) on the other. The DL/RL networks and learning algorithms ("Learners") provide us with instances of domain-general, sample-inefficient learning systems, while the meta-trained LSTMs provide us with instances of domain-specific, but sample-efficient learning systems. We refer to these LSTMs as "Meta-Learners", though we focus primarily on their inner loop of learning, after significant outer-loop training (i.e., after meta-learning) has occurred.

While previous effort has highlighted the sample efficiency, convergence, and generalisation properties of meta-learning systems (e.g. Baxter, 1998; 2000; Hochreiter et al., 2001; Vinyals et al., 2016; Santoro et al., 2016; Finn et al., 2017; Amit and Meir, 2018; Grant et al., 2018), we explicitly factor these out. Instead, we consider whether Learners and Meta-Learners pursue the same *learning trajectory*, i.e., whether they incrementally capture the same structure while learning the task.

To do this, we apply Learners and Meta-Learners to a series of three simple, structured tasks, within which the learning dynamics of Learners have been theoretically and empirically characterised (Saxe et al., 2013; Rahaman et al., 2018; Xu et al., 2018; Schaul et al., 2019). In each case, we measure whether the biases that Learners show during their learning process also manifest within Meta-Learners' learning process. In all three cases we find that they do not.

This work is relevant for several reasons. First, it gives us an indication of how different learning systems operate when they are not yet trained to convergence. While it is common practice to describe how learning systems behave once they have reached "equilibrium" (i.e., once training has converged), there are various reasons why we should anticipate ML systems will be deployed before reaching their theoretically-optimal performance. Most notably, real-world optimisation takes place under the con-

straints of finite resources, including finite compute and limited time. Moreover, we typically do not have the luxury of knowing exactly how far a given solution to a complex task is from the global optimum. A rich characterisation of how far learning systems progress on a resource budget gives us an indication of the kinds of errors that we should anticipate that they would make. Information we glean here could be valuable when evaluating the safety of deployed systems.

In addition to this, we add to the growing literature on how learning systems can build abstraction layers. In particular, previous work on meta-learning has shown how sample-inefficient "outer optimisers" can build sample-efficient "inner optimisers", and how the outer optimisers can draw from task information to bake novel priors into the inner ones (Rendell et al., 1987; Thrun, 1998; Giraud-Carrier et al., 2004; Ravi and Larochelle, 2017; Grant et al., 2018; Amit and Meir, 2018; Harrison et al., 2018). Our contribution to this literature is to demonstrate an analogous phenomenon with the learning process itself: outer optimisers can configure inner optimisers to pursue *learning trajectories* less available to a non-nested system.

Through this, our work puts into perspective previous research on the learning dynamics of neural network systems. It is tempting to interpret previous analyses (e.g. Saxe et al., 2013; Arpit et al., 2017; Rahaman et al., 2018; Xu et al., 2018) as revealing something fundamental about neural networks' learning behaviour, for example, that neural networks will always learn the "most important", "dominant", or "simple" structure present in a task first. Our results show that these results are not as universal as they first seemed, as learning dynamics are also a function of the priors that a learner brings to a task.

The remainder of this document proceeds as follows. In Section 2, we briefly review relevant work on learning dynamics, meta-learning, and the particular distinctions which have been made between Learners' and Meta-Learners' behaviours. We then walk through three experiments in turn. In Section 3, following previous work of Saxe et al. (2013), we consider the learning dynamics of deep networks on linear regression tasks. In Section 4, following previous work of Rahaman et al. (2018) and Xu et al. (2018), we consider the learning dynamics of deep networks on nonlinear regression tasks. Finally, in Section 5, following previous work of Schaul et al. (2019), we consider the dynamics of reinforcement learning, specifically an interference phenomenon that occurs during on-policy learning of contextual policies. We conclude in Section 6 by characterising the outer learning dynamics by which the Meta-Learners are themselves configured.

2. Related work

There is a long history of interest in the learning dynamics of neural networks equipped with SGD and its variants ("Learners", by our terminology). The field's principal goal in studying this has been to improve optimisation techniques. Many studies have thus investigated the learning process to extract convergence rates and guarantees for various optimisers, and well as to identify properties of optimisation landscapes for canonical tasks (Bottou, 2010; Dauphin et al., 2014; Su et al., 2014; Choromanska et al., 2015; Goodfellow et al., 2014; Schoenholz et al., 2016; Wibisono et al., 2016; Li et al., 2018; Pennington et al., 2018; Yang et al., 2018; Baity-Jesi et al., 2018).

From this optimisation-centric perspective, intermediate stages of learning are generally viewed as obstacles to be overcome. As gradient descent methods are typically conceived as a local search in a hypothesis space, the point of learning is to find a better hypothesis than the current one. Thus one considers the gradient that takes one *away* from the current parameters, how one can *escape* from saddle points, and how to avoid *getting stuck* in local minima or boring plateaux. Intermediate parameters (and their corresponding hypotheses) are rarely points of interest in and of themselves. This view is reflected in the standard procedure of plotting and presenting graphs of how loss decreases over the course of training, which reinforces the conception that the defining characteristic of an intermediate stage of learning is that it is not yet the end.

There have been a few notable areas of research where this conception has been openly challenged.

First, there have been efforts to characterise when *particular* task substructures are learned during training. We take several of these as our starting point for investigation of sample-efficient learning dynamics, which are discussed throughout the text (Saxe et al., 2013; Rahaman et al., 2018; Xu et al., 2018; Schaul et al., 2019). We note three more cases from the supervised image classification literature. Arpit et al. (2017) studied the order in which labels are learned by classifiers, finding that inputs with randomised labels are learned later than those with correct labels. Achille et al. (2019) observed that certain structure could only be efficiently learned early in training, reminiscent of the phenomenon of critical periods in biological learning (Hensch, 2004), while Toneva et al. (2018) found that the predicted labels for some inputs are regularly forgotten by many learners over the course of training, which the authors relate to the gradual construction of a maximum margin classifier (Soudry et al., 2018). There have likewise been several studies which have drawn attention to how various statistics change over the course of learning, such as representational geometry (e.g. Raghu et al., 2017), information geometry (e.g. Shwartz-Ziv and Tishby, 2017;

Achille and Soatto, 2018; Chaudhari and Soatto, 2018; Saxe et al., 2018b), and generalisation (e.g. Prechelt, 1998; Advani and Saxe, 2017; Lampinen and Ganguli, 2018).

Second, learning dynamics are a central focus in the field of curriculum learning (Elman, 1993; Bengio et al., 2009; Weinshall and Amir, 2018), where it is necessary to identify what a learner has and has not yet grasped in order to select data for the next stage for training.

Finally, the intermediate behaviour of learners plays a crucial role in reinforcement learning (as well as the more general field of active learning (Lewis and Gale, 1994; Cohn et al., 1996; Settles, 2012)). Here there exists a feedback loop between the current stage of learning (in RL, via the policy) and the data distribution being trained on. An agent's behaviour during intermediate stages of learning is directly responsible for generating the opportunities to change the policy. This is a core reason for the critical research agenda on deep exploration (e.g. Jaksch et al., 2010; Osband et al., 2016; Houthooft et al., 2016; Pathak et al., 2017; Tang et al., 2017; Fortunato et al., 2017).

Aside from related work on learning dynamics, this paper connects to a literature that is beginning to probe the behaviour of meta-learners. There now exists a range of novel meta-learning systems that exploit memory-based networks (Hochreiter et al., 2001; Santoro et al., 2016; Wang et al., 2016; Duan et al., 2016; Mishra et al., 2017)—such as the LSTM Meta-Learners we consider here—as well as gradient-based inner optimisation (Finn et al., 2017; Rusu et al., 2018), evolution (Hinton and Nowlan, 1987; Fernando et al., 2018), and learned optimisers (Andrychowicz et al., 2016; Chen et al., 2017; Li and Malik, 2016; Ravi and Larochelle, 2017), with a range of applications that are too numerous to survey here. To the best of our knowledge, however, comparatively less work has been done to explore the detailed manner in which the meta-learned learners progressively acquire mastery over task structure during an episode. Several papers have identified relationships between meta-learners' inner learning processes and Bayes-optimal algorithms, either empirically (Kanitscheider and Fiete, 2017; Chen et al., 2017; Rabinowitz et al., 2018), or theoretically (Baxter, 1998; 2000; Grant et al., 2018). Some work has been done to explore how the behaviour of these systems changes over the course of inner learning in specific domains: Wang et al. (2016) identified the adoption of different effective learning rates in meta-reinforcement learning; Eslami et al. (2018), Rabinowitz et al. (2018), and Garnelo et al. (2018) characterised how inner learners' uncertainty decreases over inner learning in networks trained on conditional scene generation, intuitive psychology, and GP-like prediction respectively; while Kanitscheider and Fiete (2017) and Gupta et al. (2018) characterised inner exploration policies (and

the limits thereof (Dhiman et al., 2018)). Our work adds to this literature by empirically characterising inner learners' learning process on simple problems with clear known structure, and differentiating these dynamics from those of DL and RL Learners.

Finally, a goal of this work is to provide clear examples of how *sample-inefficient* learning may, at the behavioural level, look radically different from *sample-efficient* learning. This links directly to the question of how we should relate machine learning to human learning. The manner in which humans learn has long served as core inspiration for building machine learning systems (Turing, 1950; Rosenblatt, 1958; Schank, 1972; Fukushima and Miyake, 1982), and remains an aspirational standard for much of AI research (e.g. Mnih et al., 2015; Lake et al., 2015; Vinyals et al., 2016; Lake et al., 2017). This, of course, applies to many of the core learning paradigms, whose origins can be traced in part to settings in which humans learn, such as supervised learning (Rosenblatt, 1958), unsupervised learning (Hebb et al., 1949; Barlow, 1989; Hinton et al., 1986), reinforcement learning (Thorndike, 1911; Sutton and Barto, 1998), imitation learning (Piaget, 1952; Davis, 1973; Galef Jr, 1988; Hayes and Demiris, 1994; Schaal et al., 2003), and curriculum learning (Elman, 1993). But there has also long been a desire to connect human and machine learning at a finer grain. Early connectionist models proposed relationships between the dynamics of human learning during development and the dynamics of artificial neural networks during training (Plunkett and Sinha, 1992; McClelland, 1995; Rogers and McClelland, 2004; Saxe et al., 2018a). Notwithstanding prevailing discussions about whether the mechanisms of backpropagation are biologically plausible (Crick, 1989; Stork, 1989; Lillicrap et al., 2016; Marblestone et al., 2016; Guerguiev et al., 2017), the idea that humans and machines may show similar learning dynamics at a *behavioural* level remain current, with parallels recently being proposed for perceptual learning (Achille et al., 2019) and concept acquisition (Saxe et al., 2018a). Moreover, a number of similarities have been identified between the *representations* produced by machine and human learning (e.g. Olshausen and Field, 1996; Yamins et al., 2014; Khaligh-Razavi and Kriegeskorte, 2014; Güçlü and van Gerven, 2015; Nayebi et al., 2018; Yang et al., 2018). This line of research is suggestive that there may exist a level of abstraction within which the dynamical processes of deep learning and human learning align.

Despite this argument, there remain huge points of difference between how we and current deep learning systems learn to solve many of the tasks we face. Lake et al. (2017) constructs a sweeping catalogue of these, highlighting, most relevantly here, humans' sample-efficiency, as well as features of the solutions we produce such as their

generalisability, deployment of causality, and compositionality. As the ML community increasingly innovates on techniques that yield more sample-efficient learning in specialised domains, our contribution to this field lies in raising the hypothesis: when humans and machines learn with radically different sample efficiencies, their *learning trajectories* may well end up being very different.

3. Experiment 1: Linear regression

In our first experiment, we study a phenomenon originally described by Saxe et al. (2013), and extended in a number of subsequent studies (Advani and Saxe, 2017; Saxe et al., 2018a; Stock et al., 2018; Bernacchia et al., 2018; Lampinen and Ganguli, 2018). These results begin with an analytic demonstration that when one trains deep linear networks on linear regression problems using stochastic gradient descent (SGD), they learn the target function with a stereotyped set of dynamics.

More precisely, we define the target regression problem to be of the form $\boldsymbol{y} = \boldsymbol{W}\boldsymbol{x} + \boldsymbol{\varepsilon}$, where $\boldsymbol{\varepsilon} \sim \mathcal{N}(\boldsymbol{0}, \boldsymbol{\Sigma_\varepsilon})$. A deep linear network is a feedforward network without any nonlinearities, parameterised by a set of weight matrices $\boldsymbol{W_i}$, and whose outputs are of the form $\hat{\boldsymbol{y}} = \left(\prod_{i=1}^{n} \boldsymbol{W_i}\right)\boldsymbol{x}$. Given this setup, Saxe et al. (2013) showed that over the course of training, the network will learn the singular modes of $\boldsymbol{W}$ in order of their singular values. Thus, if we define the singular value decomposition (SVD) of the target matrix via $\boldsymbol{W} = \boldsymbol{USV}^\top = \sum_i s^{(i)} \boldsymbol{u}^{(i)} \boldsymbol{v}^{(i)\top}$, then the time course of learning of each singular mode, $\boldsymbol{u}^{(i)} \boldsymbol{v}^{(i)\top}$, is sigmoidal, with a time constant inversely proportional to the singular value $s^{(i)}$. In both this, and subsequent work, it was shown empirically that these results extend to the training of deep nonlinear networks using stochastic gradient descent.

In what follows, we first replicate empirical results for an SGD-based deep Learner for completeness (Section 3.1), setting up the standard experimental parameters and protocols. We then consider the dynamics by which a sample-efficient Meta-Learner—trained to learn linear regression problems—acquires structure while learning problems of the same form (Section 3.2). We save analysis of the learning process by which the Meta-Learner itself is constructed to Section 6.

3.1. Learner

3.1.1. SETUP

We consider linear regression problems of the form $\boldsymbol{y} = \boldsymbol{W}\boldsymbol{x} + \boldsymbol{\varepsilon}$, where $\boldsymbol{x} \in \mathbb{R}^{N_x}$ and $\boldsymbol{y}, \boldsymbol{\varepsilon} \in \mathbb{R}^{N_y}$. We run experiments both where $N_x = N_y = 2$ and $N_x = N_y = 5$ (i.e., 2D and 5D respectively). In all cases, we use isotropic

noise, with $\boldsymbol{\varepsilon} \sim \mathcal{N}(\boldsymbol{0}, 0.01^2 \boldsymbol{I})$.

We train Learners on a single task, defined by sampling a random ground-truth weight matrix $\boldsymbol{W}$ with a fixed spectrum. To do this, we sample a matrix from the zero-mean, isotropic matrix-normal distribution $\mathcal{MN}(\boldsymbol{0}, \boldsymbol{I}, \boldsymbol{I})$, compute its SVD, then replace the spectrum with the desired one. This weight matrix is then held fixed for the duration of training. All data is procedurally-generated (i.e., there is no fixed training set), with inputs $\boldsymbol{x} \sim \mathcal{N}(\boldsymbol{0}, \boldsymbol{I})$.

For our Learners, we use 2-layer linear MLPs equipped with SGD, the details of which can be found in Appendix A.1. The objective, as standard, is to minimise the l_2 loss between the network's prediction, $\hat{\boldsymbol{y}}$, and the target, $\boldsymbol{y}$. As per previous work (Saxe et al., 2013; Advani and Saxe, 2017; Lampinen and Ganguli, 2018), there are a wide range of deep network architectures and initialisations under which the same results hold, and we find our results similarly robust.

3.1.2. HOW TO ASSESS LEARNING DYNAMICS

Since we are interested in the learning dynamics of the network, we use the subscript t to denote the training step. Writing the output of the ($L = 2$ layer) network at step t as:

$$\hat{\boldsymbol{y}_t} = \left(\prod_{l=1}^{L} \boldsymbol{W}_{l,t}\right)\boldsymbol{x} \tag{1}$$

$$= \hat{\boldsymbol{W}_t}\boldsymbol{x} \tag{2}$$

we obtain the effective linear function executed by the network at this training step as $\hat{\boldsymbol{W}_t}$. We then project the effective linear weight matrix, $\hat{\boldsymbol{W}_t}$, onto the coordinate system induced by the SVD of the target weight matrix, $\boldsymbol{W}$. If we write the decomposition as $\boldsymbol{W} = \boldsymbol{USV}^\top$, then the spectrum of $\boldsymbol{W}$ can be expressed as $\boldsymbol{s} = \mathrm{diag}(\boldsymbol{U}^\top \boldsymbol{W} \boldsymbol{V})$. Thus, to determine the effective progress at training step t, we compute the network's *effective spectrum*:

$$\hat{\boldsymbol{s}}_t = \mathrm{diag}\left(\boldsymbol{U}^\top \hat{\boldsymbol{W}_t} \boldsymbol{V}\right) \tag{3}$$

We ignore the non-diagonal terms, which carry residuals not aligned to the target task's singular modes. In what follows, we primarily consider the learning dynamics of individual singular modes, $\hat{s}_{k,t}$ (where k indexes the mode), rather than the learning dynamics of joint spectra.

3.1.3. RESULTS

Fig 1a shows the Learner's learning dynamics for individual singular modes. As per Saxe et al. (2013), singular modes of $\boldsymbol{W}$ with large singular values (darker colours, larger asymptotic values) are learned faster, i.e.
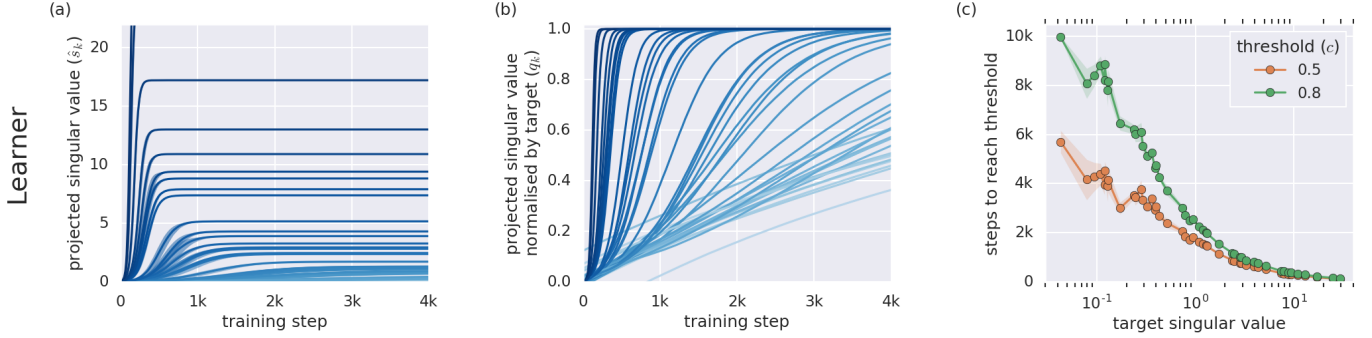
Figure 1. **(a)** Learning dynamics of the Learner ($\hat{s}_{k,t}$) for singular modes of different singular values. Modes with larger singular values are darker, and converge faster, as per Saxe et al. (2013). Data are accrued from a number of Learners trained on different 2D regression problems with a range of target spectra. **(b)** As in (a), but showing proportions of the target value, $q_k(t) = \hat{s}_{k,t}/s_k$. This makes the difference in learning speed more visible. **(c)** Training steps required for the Learner to reach a threshold of performance where $q_k(t) > c$, for different cutoff values c. This demonstrates that the learning speed of singular modes is slower for smaller singular values. Shaded areas here, and in the rest of the paper, denote standard errors across networks.

with sigmoidal learning curves that converge quicker. Conversely, singular modes with smaller singular values (lighter colours, smaller asymptotic values) are learned slower. These dynamics are even more visible when we primarily consider the learned singular values as a proportion of the target singular value, $q_k(t) = \hat{s}_{k,t}/s_k$, in Fig 1b. Finally, we quantify the learning rate of these singular modes by measuring the number of training steps it takes for the learned singular modes to reach a threshold proportion of the target value, $q_k(t) > c$, in Fig 1c. Here it can be seen that the larger the value of the singular mode to be estimated, the fewer steps it takes.

Similar results are shown for the 5D case in Appendix Fig A1a, and for nonlinear deep nets in Appendix Fig A2.

3.2. Meta-Learner

3.2.1. SETUP

We sought to compare these learning dynamics with those of a sample-efficient meta-learner, which had been explicitly configured to be able to learn new linear regression problems.

To do this, we ("outer"-)trained an LSTM Meta-Learner (architecture details in Appendix A.2), using the same rough procedure as Hochreiter et al. (2001) and Santoro et al. (2016), as follows.

On each length-T episode i during outer-training, we presented the Meta-Learner with a *new* regression problem, by sampling a new target weight matrix $\boldsymbol{W}^{(i)}$. We then sampled a sequence of inputs, $\{\boldsymbol{x}_t^{(i)}\}_{t=1}^{T}$, where each $\boldsymbol{x}_t^{(i)} \sim \mathcal{N}(\boldsymbol{0}, \boldsymbol{I})$ for each time step $t \in \{1, ..., T\}$. In turn, we computed the corresponding targets, $\boldsymbol{y}_t^{(i)} = \boldsymbol{W}^{(i)}\boldsymbol{x}_t^{(i)} + \boldsymbol{\varepsilon}_t^{(i)}$,

with each $\boldsymbol{\varepsilon}_t^{(i)} \sim \mathcal{N}(0, 0.01^2\boldsymbol{I})$.

At each time point t in the episode, the objective of the LSTM Meta-Learner is to predict the target $\boldsymbol{y}_t^{(i)}$, given $\boldsymbol{x}_t^{(i)}$ and the history of previous inputs and targets, $\{(\boldsymbol{x}_{t'}^{(i)}, \boldsymbol{y}_{t'}^{(i)})\}_{t'=1}^{t-1}$. We implement this by feeding into the LSTM at time t a concatenation of $\boldsymbol{x}_t^{(i)}$ and $\boldsymbol{y}_{t-1}^{(i)}$ (setting $\boldsymbol{y}_0^{(i)} = \boldsymbol{0}$), and linearly reading out a prediction $\hat{\boldsymbol{y}}_t^{(i)}$ from the LSTM at the same time step.

To outer-train the LSTM itself, we minimised the average of the l_2 losses over the course of the episode, i.e., the quantity:

$$\mathcal{L}^{(i)} = \frac{1}{T} \sum_{t=1}^{T} ||\hat{\boldsymbol{y}}_t^{(i)} - \boldsymbol{y}_t^{(i)}||^2 \qquad (4)$$

using BPTT and episode lengths of $T = 20$. During this outer-training process, we sampled target weight matrices from a fixed distribution. Unless stated otherwise, we used a standard matrix-normal distribution, with $\boldsymbol{W}^{(i)} \sim \mathcal{MN}(\boldsymbol{0}, \boldsymbol{I}, \boldsymbol{I})$. For consistency between the outer-learning algorithm and the Learner described in the previous Section, we trained the Meta-Learner with SGD.

3.2.2. INNER AND OUTER LEARNING DYNAMICS

We note that the Meta-Learner has *two* learning dynamics: the *inner dynamics* by which the configured LSTM learns a solution to a new regression problem; and the *outer dynamics* by which the LSTM itself is shaped in order to be able to do regression at all. While the inner learning dynamics are sample efficient and occur through changes in the LSTM's activations, the outer learning dynamics are sample inefficient and occur through changes in the LSTM's

weights.

Our primary focus in this manuscript is a comparison between how two learning systems approach single regression problems. As such, we concentrate here on the inner dynamics of the Meta-Learner, once outer-training has produced a sufficiently performant system. This allows us to make direct comparison between the process by which sample-inefficient Learners and sample-efficient Meta-Learners come to discover and capitalise on structure in the same learning task. We leave all analysis of outer-loop behaviour to Section 6.

3.2.3. HOW TO ASSESS LEARNING DYNAMICS

We thus consider here a Meta-Learner LSTM with fixed weights. Our goal is to estimate the effective function realised by the LSTM at iteration t of an episode i, which we denote $\hat{g}_t^{(i)} : \mathbb{R}^{N_x} \to \mathbb{R}^{N_y}$, and determine how this function changes with more observations (i.e., as t increases).

We begin by sampling a target weight matrix for the episode, $\boldsymbol{W}^{(i)}$, with a spectrum of interest. For each time point, t, we sample a *fixed* sequence of prior observations, $\{ \left(\boldsymbol{x}_{t'}^{(i)}, \boldsymbol{y}_{t'}^{(i)} \right) \}_{t'=1}^{t-1}$. Using this sequence to determine the LSTM's hidden state, we then compute a linear approximation of $\hat{g}_t^{(i)}(\cdot)$ as follows: we sample a probe set of N different values of $\boldsymbol{x}_t^{(i)}$ from $\mathcal{N}(\boldsymbol{0}, \boldsymbol{I})$; compute the respective values of $\hat{\boldsymbol{y}}_t^{(i)}$; and use linear least squares regression on this probe set to approximate $\hat{\boldsymbol{y}}_t^{(i)} \approx \hat{\boldsymbol{W}}_t^{(i)} \boldsymbol{x}_t^{(i)}$.

We focus our attention on how the estimates $\hat{\boldsymbol{W}}_t^{(i)}$ project onto the singular modes of the episode ground-truth matrix $\boldsymbol{W}^{(i)} = \boldsymbol{U}^{(i)} \boldsymbol{S}^{(i)} \boldsymbol{V}^{(i)\top}$, via the effective spectra:

$$\hat{\boldsymbol{s}}_t^{(i)} = \mathrm{diag} \left(\boldsymbol{U}^{(i)\top} \hat{\boldsymbol{W}}_t^{(i)} \boldsymbol{V}^{(i)} \right) \qquad (5)$$

By tracking the effective spectra over the course of (inner) learning, we obtain an analogous measurement to that computed for the Learner in Equation (3).

For each time, t, and episode i, we use $N = 100$ samples to estimate $\hat{\boldsymbol{W}}_t^{(i)}$, all with the same fixed sequence of prior observations. When studying the learning dynamics for particular target spectra, we sample new target matrices $\boldsymbol{W}^{(i)}$ with the same spectra, and for each, compute the inner dynamics over which the singular values are learned (using new input samples as well). For each time, t, we average the effective spectra, $\hat{\boldsymbol{s}}_t^{(i)}$ over 100 episodes (where each episode has the same target spectrum, $\boldsymbol{s}^{(i)}$, but uniquely-rotated target matrices and unique input sequences) and report statistics over 10 independently-trained instances of Meta-Learner LSTMs.

3.2.4. RESULTS: IN-DISTRIBUTION

The Meta-Learner is outer-trained on weight matrices drawn from the standard matrix normal distribution. This induces a particular distribution over singular values, shown in Fig 2. We concentrate first on the Meta-Learner's learning behaviour for singular values up to the 95th percentile of this distribution. Learning on more extreme singular values (which we consider out-of-distribution) is characterised in Section 3.2.5 below.

Fig 3 shows the Meta-Learner's learning dynamics for individual singular modes, in the same form as Fig 1. We note two major differences. First, as expected, the Meta-Learner is dramatically more sample efficient than the Learner (by a factor of $\mathcal{O}(1000)$). However, when we factor this out, we see a second important difference: the Meta-Learner does *not* show the Learner's pattern of learning singular modes with large singular values faster. Rather, the Meta-Learner learns all in-distribution singular modes at roughly the same rate.

Putting these changes into perspective, a $50\times$ decrease in a mode's singular value causes the Learner to take roughly $9\times$ as long to learn it, while it causes the Meta-Learner to take only $1.05\times$ as long.

We show similar results for 5D matrices ($N_x = N_y = 5$) in the appendix, as Figs A1b-c.

An instructive way to view the difference between the Learner's behaviour and the Meta-Learner's is through the evolution of the effective spectrum over the course of training. In this way, one can consider Learners and Meta-Learners at equal levels of performance, and compare what components of the task they have captured at this stage of learning. We show this in Fig 4 for a 5D linear regression problem. Here it can be clearly seen how the Learner acquires the dominant singular structure first, while the Meta-Learner acquires all the singular structure concurrently.

3.2.5. RESULTS: OUT-OF-DISTRIBUTION

As mentioned above, the Meta-Learner is outer-trained on matrices with a particular distribution of singular values. When we step outside this—by presenting the Meta-Learner with a target matrix with singular modes greater than the 95th percentile—the Meta-Learner progressively fails to learn the full extent of the singular mode (Fig 5).

One potential cause of this behaviour is saturation of the LSTM outside of its natural operating regime when the target outputs are too large. However, this regime is an (outer) learned property: when we outer-train the Meta-Learner on weight matrices from a scaled matrix normal distribution, with $\boldsymbol{W}^{(i)} \sim \mathcal{MN}(\boldsymbol{0}, \alpha^2 \boldsymbol{I}, \alpha^2 \boldsymbol{I})$, the patterns seen in Fig 5 shift approximately to match the scale of singular
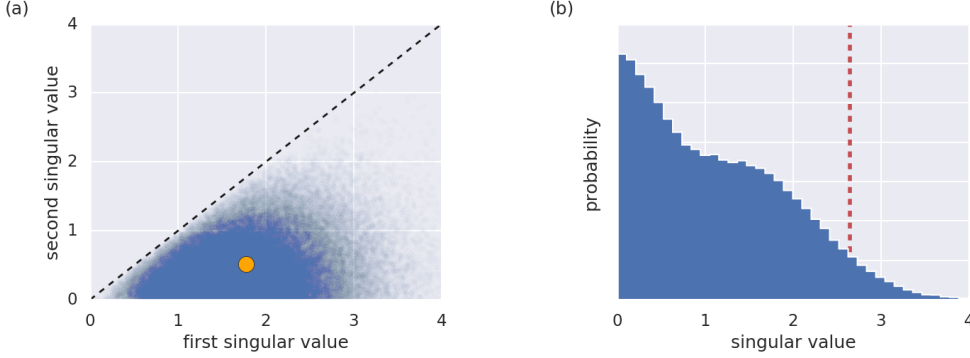
6

Figure 2. **(a)** Samples from the joint distribution over first and second singular values for 2×2 matrices $\boldsymbol{W}^{(i)} \sim \mathcal{MN}(\boldsymbol{0}, \boldsymbol{I}, \boldsymbol{I})$. Orange dot shows mean spectrum. **(b)** Marginal distribution of all singular values. Red vertical line shows the 95th percentile.
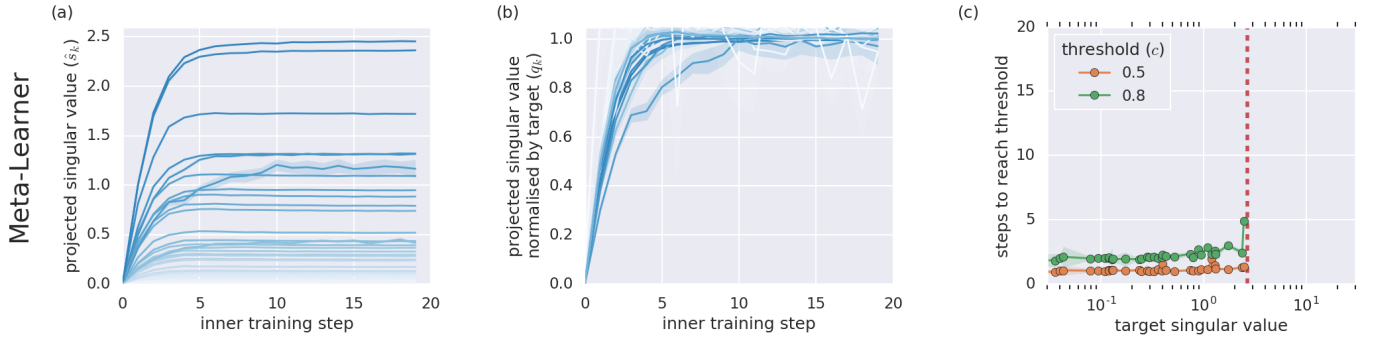

Figure 3. Learning dynamics of the Meta-Learner for singular modes of different singular values, as in Fig 1.

modes within the distribution (e.g. Fig A3).

Congruent with this hypothesis, the Meta-Learner was generally competent at learning singular values *smaller* than a lower cutoff of the outer-training distribution. When we outer-trained the Meta-Learner on more exotic distributions of matrices—such as enforcing the distribution of singular values to be uniform over a range $[s_{\min}, s_{\max}]$—the Meta-Learner was equally fast (and competent) at learning singular values smaller than $s_{\min}$ as those within $[s_{\min}, s_{\max}]$.

Finally, one might ask whether the difference in learning dynamics between the Learner and Meta-Learner are due to different parameterisations: while the Learner uses a feedforward network, the Meta-Learner uses an LSTM. To test this hypothesis, we trained a Learner using the same LSTM architecture as the Meta-Learner (albeit solving a single linear regression problem only, i.e. one where the target matrix is always the same across episodes). This did not qualitatively affect the learning dynamics of the Learner (Fig A4).

3.2.6. RELATIONSHIP TO BAYES-OPTIMAL INFERENCE

A number of links have been drawn between meta-learning and Bayes-optimal inference, in particular, that over outer-training, the inner loop should come to approximate amortised Bayes-optimal inference (Baxter, 1998; 2000; Grant et al., 2018). Indeed, we show here that Bayes-optimal inference follows the same qualitative learning dynamics as the Meta-Learner on solving new (in-distribution) linear regression problems.

We assume we have a Bayes-optimal observer performing multivariate inference, with the correct prior over $\boldsymbol{W}$, $P(\boldsymbol{W}) = \mathcal{MN}(\boldsymbol{0}, \boldsymbol{I}, \boldsymbol{I})$, and the correct ground-truth noise covariance, $\boldsymbol{\Sigma_\varepsilon} = \sigma_\varepsilon^2 \boldsymbol{I}$. Given this, the posterior over $\boldsymbol{W}$ after t observations takes the form (Bishop, 2006):

$$P(\boldsymbol{W}|\boldsymbol{Y_t}, \boldsymbol{X_t}) = \mathcal{MN}(\bar{\boldsymbol{W}}_t, \boldsymbol{\Lambda_t^{-1}}, \sigma_e^2 \boldsymbol{I}) \quad (6)$$
$$\bar{\boldsymbol{W}}_t = (\boldsymbol{X_t^\top X_t} + \sigma_e^2 \boldsymbol{I})^{-1} \boldsymbol{X_t^\top Y_t} \quad (7)$$
$$\boldsymbol{\Lambda_t} = \boldsymbol{X_t^\top X_t} + \sigma_e^2 \boldsymbol{I} \quad (8)$$

where $\boldsymbol{X_t}$ and $\boldsymbol{Y_t}$ are matrices of t observed inputs and outputs respectively.

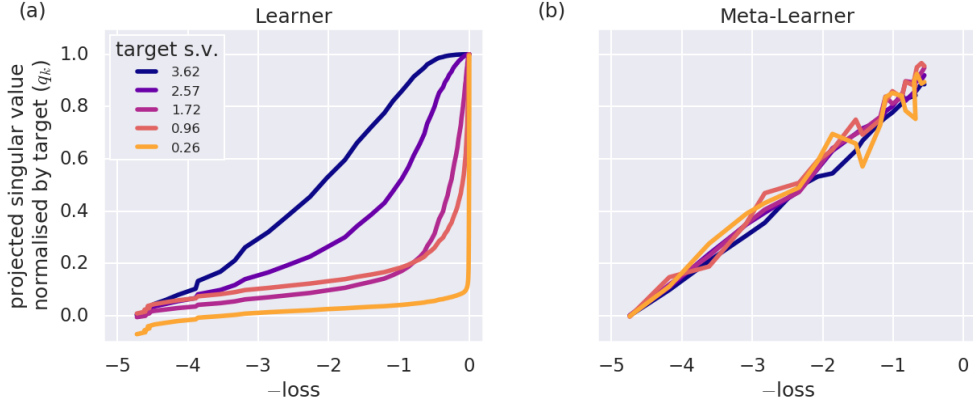In Fig 6, we show how the posterior mean, $\bar{\boldsymbol{W}}_t$, evolves

Figure 4. Effective spectrum of a 5D linear regression problem over the course of training, for **(a)** the Learner, and **(b)** the Meta-Learner. The x-axes show training progress (shown as the negative of the loss), which improves as one moves rightwards. Colours show the learning progress of each singular mode, as the proportion of the target value, $q_k(t)$. Results are shown averaged over 100 target matrices $\boldsymbol{W}^{(i)}$, all of which have the same spectrum (which we selected as the expected spectrum of matrices drawn from $\mathcal{MN}(\boldsymbol{0}, \boldsymbol{I}, \boldsymbol{I})$).
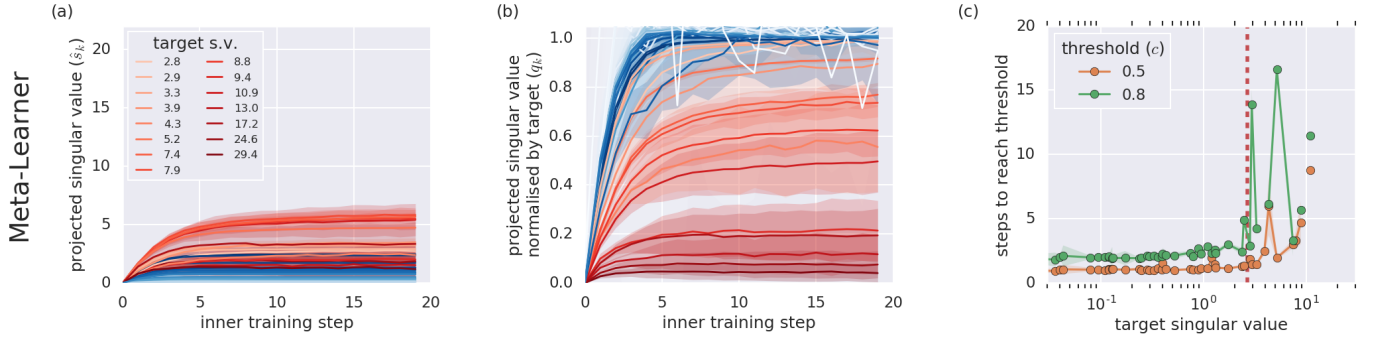
Figure 5. Learning dynamics of the Meta-Learner for singular modes of different singular values, as in Fig 3. Blue lines in (a) and (b) are the dynamics of learning for within-distribution singular values, as in Fig 3; red lines show learning of out-of-distribution singular values. Red vertical line in (c) shows the 95th percentile of the distribution of singular values, as in Fig 2b.

over training, via its (expected) spectrum. This algorithm learns all singular values concurrently, much like the pattern observed in the Meta-Learner.

3.3. The choice of optimiser

How dependent are these results on the underlying optimisation algorithm in use? The experiments presented so far were all performed using an SGD optimiser, which the Learner deployed directly in service of the regression task at hand, and which the Meta-Learner deployed during outer training.

We repeated the same experiments using the Adam optimiser (Kingma and Ba, 2014). While this changed the Learner's speed of learning *across* regression problems—such that tasks with a larger norm of the matrix $\boldsymbol{W}$ were slower to learn—it did not change the general pattern of learning a *given* regression problem: the dominant singular

mode was always learned first, and smaller singular modes later (Fig 7).

We observed no qualitative effects of using Adam rather than SGD on the behaviour of the Meta-Learner.

3.4. Summary

In this section, we compared how sample-inefficient deep Learners, and sample-efficient LSTM Meta-Learners (pre-configured through meta-learning) progressively capture the structure of a linear regression task. While Learners latch on to the singular modes progressively, in order of their singular values, the sample-efficient LSTM Meta-Learners estimate all the singular modes concurrently. These latter learning dynamics are congruent with the dynamics of Bayes-optimal linear regression algorithms.
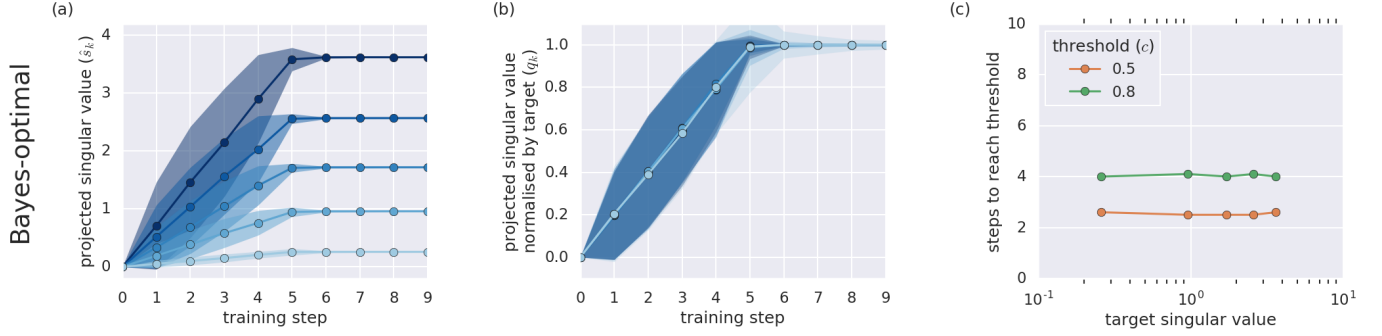
Figure 6. Learning dynamics of Bayesian multi-variate linear regression for a 5D problem (with spectrum as in Fig 4). Results shown as for Fig 3.
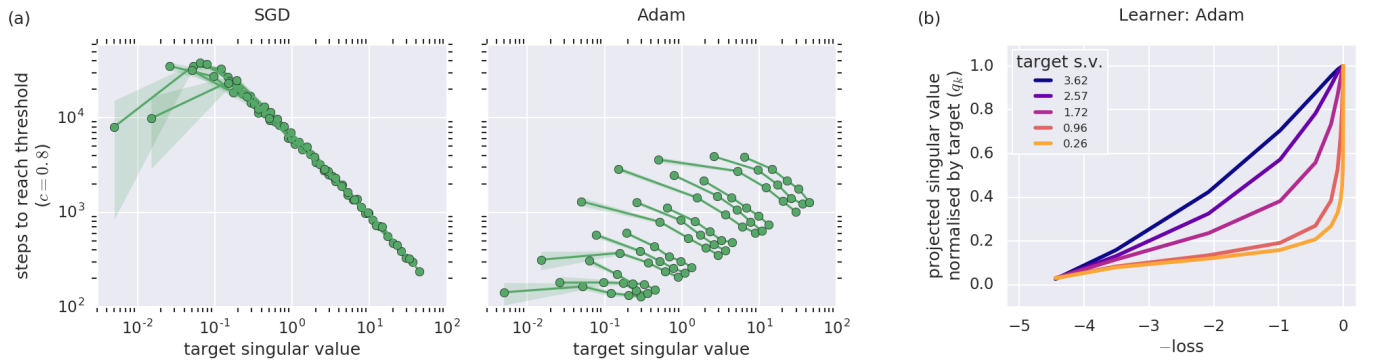

Figure 7. Learning dynamics of the Learner on 5D regression problems, when using SGD and (left) Adam optimisers (right). **(a)** Training steps to reach the 80% threshold of each singular value (i.e., for $q_k(t) > 0.8$), as in Fig 1c. Each line shows the dynamics on target matrices with a particular spectrum. Both optimisers induce the same learning dynamics on each task: the dominant singular mode is learned first. **(b)** Effective spectrum of a 5D regression problem for the Adam-based Learner, over the course of training, as in Fig 4. Note that the use of Adam maintains the staggered pattern of learning singular modes.

4. Experiment 2: Nonlinear regression

In our second experiment, we study a phenomenon reported by Rahaman et al. (2018) and Xu et al. (2018). This work demonstrates that Deep ReLU and sigmoid networks discover structure in *nonlinear* regression problems in a similarly staggered fashion: they uncover the low Fourier frequencies in the target function before the higher frequencies.

In what follows, we first replicate empirical results for a deep Learner for completeness (Section 4.1), again setting up the standard experimental parameters and protocols. As in the previous Experiment, we then consider the dynamics by which a sample-efficient Meta-Learner—outer-trained to learn nonlinear regression problems—acquires structure while learning problems of the same form (Section 4.2). Once again, we save analysis of the learning process by which the Meta-Learner itself is constructed to Section 6.

4.1. Learner

4.1.1. SETUP

We consider nonlinear regression problems of the form $y = g(x) + \varepsilon$, where $\varepsilon \sim \mathcal{N}(0, \sigma_\varepsilon^2)$. We consider here only univariate functions $g : \mathbb{R} \to \mathbb{R}$ defined over the interval $[-0.5, 0.5]$, though the theory and experiments in previous work (Rahaman et al., 2018; Xu et al., 2018; Xu, 2018) extend to the more general multivariate case (with larger support).

We train Learners on a single task, defined by sampling a scalar function g to have a (boxcar) low-pass Fourier spectrum (with a zero DC term), defined using the first $K = 5$ modes of the Fourier series:

$$g(x) = \sum_{k=1}^{5} \sin(2\pi kx + \phi_k) \qquad (9)$$

This amounts to sampling the phases $\phi_k \sim \mathcal{U}[0, 2\pi]$. This

function is then held fixed for the duration of training. All data is procedurally-generated, with $x \sim \mathcal{U}[-0.5, 0.5)$.

Details of the Learners can be found in Appendix A.3. The objective is to minimise the l_2 loss between the network's prediction $\hat{y}$ and the target y.

4.1.2. HOW TO ASSESS LEARNING DYNAMICS

At each training step, t, we estimate the effective function represented by the Learner by feeding in a probe minibatch, $\boldsymbol{x_{\text{probe}}}$, comprising $N = 40$ equispaced x values over the $[-0.5, 0.5)$ interval[1]. From the network's set of outputs, $\hat{\boldsymbol{y_t}}$, we compute the Fourier coefficients via an FFT.

Our interest is in the relationship between the complex Fourier coefficients of the ground-truth function, $\tilde{g}_k$, and those estimated from $\hat{\boldsymbol{y_t}}$, $\hat{\tilde{g}}_{k,t}$, where k indexes the coefficient. Analogous to the projection onto singular modes computed in the first experiment, we compute the (normalised) projection of the estimated Fourier modes onto the true ones:

$$q_k(t) = \frac{\text{Re}\left(\langle \hat{\tilde{g}}_{k,t}, \tilde{g}_k \rangle\right)}{|\tilde{g}_k|^2} \qquad (10)$$

where $\langle f, g \rangle = f g^*$ is the complex inner product. This value of $q_k(t)$ approaches one when both the amplitude and the phase of the learned Fourier modes approach those of the true Fourier modes[2].

4.1.3. RESULTS

Figs 8a-b show the Learner's learning dynamics for individual frequencies. As per Rahaman et al. (2018) and Xu et al. (2018), lower-frequency Fourier modes of g (darker colours in Fig 8b) are learned faster, i.e. with learning curves that converge quicker. Conversely, higher-frequency Fourier modes of g (lighter colours in Fig 8b) are learned slower. As in the previous section, we quantify the learning rate of these Fourier modes by measuring the number of training steps it takes for the learned modes to reach a threshold proportion of the target signal, $q_k(t) > c$, as in Fig 1c. Here it can be seen that the higher the frequency of the Fourier mode, the more steps it takes.

4.2. Meta-Learner

4.2.1. SETUP

We sought to compare these learning dynamics with those of a sample-efficient meta-learner, which had been explic-

itly configured to be able to learn new nonlinear regression problems.

To do this, we repeated the same experiment as in the previous Section, but now with LSTM Meta-Learners outer-trained on nonlinear regression problems (architecture details in Appendix A.4).

On each length-T episode i during outer-training, we presented the Meta-Learner with a new nonlinear regression problem, by sampling a new target function $g^{(i)}$. Each function had the same target Fourier spectrum [3], but different phases, $\phi_k^{(i)}$. We again sampled a sequence of inputs, $\{x_t^{(i)}\}_{t=1}^T$, where each $x_t^{(i)} \sim \mathcal{U}[-0.5, 0.5)$ for each time step $t \in \{1, ..., T\}$. In turn, we computed the corresponding targets, $y_t^{(i)} = g^{(i)}(x_t^{(i)}) + \varepsilon_t^{(i)}$. The remainder of the setup was otherwise as described in Section 3.2.1. We used episode lengths of $T = 40$.

4.2.2. HOW TO ASSESS LEARNING DYNAMICS

We consider the inner dynamics here, by which the configured LSTM learns a solution to a new nonlinear regression problem. We leave analysis of outer-loop behaviour to Section 6.

Our goal is to estimate the effective function realised by the LSTM at iteration t of an episode i, which we denote $\hat{g}_t^{(i)} : \mathbb{R} \to \mathbb{R}$, and determine how this function changes with more observations (i.e., as t increases). In particular, our interest is in the Fourier coefficients of $\hat{g}_t^{(i)}(\cdot)$, and how these compare to the Fourier coefficients of the target function $g_t^{(i)}(\cdot)$.

Our procedure for doing this is analogous to that described for the linear regression Meta-Learner, described in Section 3.2.3. For this nonlinear case, the probe set of inputs at each time point t was the equispaced minibatch $\boldsymbol{x_{\text{probe}}}$ as described in Section 4.1.2; we then apply an FFT to the respective outputs, and compute the normalised projection as in Equation (10). For each time, t, we average the projections over 2000 episodes (each with unique phases), and report statistics over 5 independently-trained instances of Meta-Learner LSTMs.

4.2.3. RESULTS: IN-DISTRIBUTION

Fig 9 shows the Meta-Learner's learning dynamics for individual Fourier modes, in the same form as Fig 8. We notice again the same discrepancy described in the linear regression case: the Meta-Learner does *not* show the Learner's

---

[1]To ensure periodicity, we sample $N = 41$ equispaced points over $[-0.5, 0.5]$, drop the final one, and centre the values to have zero mean.

[2]We obtained similar results when we ignored the phase, and simply computed the ratio of the spectral energies for each k.

[3]We also ran experiments where the amplitudes of each Fourier mode were varied across episodes, i.e. where $g^{(i)}(x) = \sum_{k=1}^K a_k^{(i)} \sin(2\pi k x + \phi_k)$, with each $a_k^{(i)} \sim \mathcal{U}[0, 1]$. Results were qualitatively identical for these experiments.
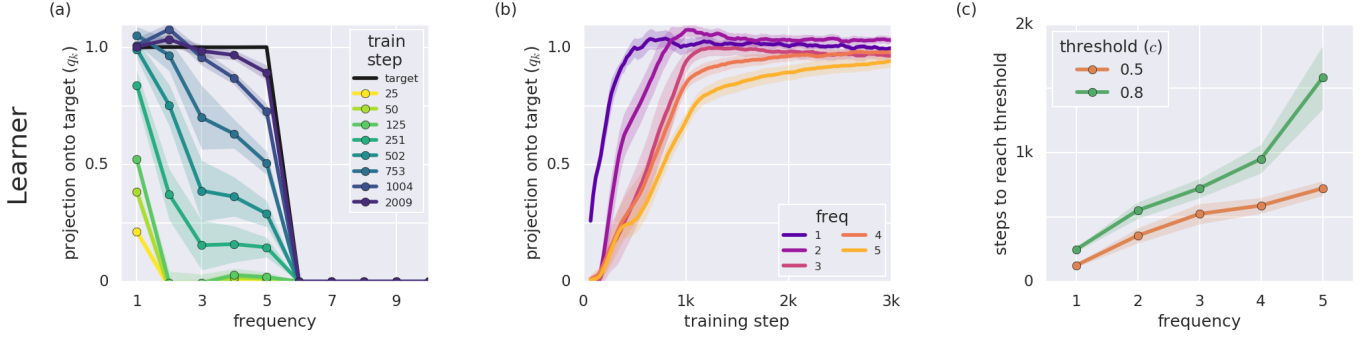
Figure 8. **(a)** Projection of the Learner's learned function onto the Fourier modes of the ground-truth function, $q_k(t)$, at different training times t. The low frequencies can be seen to converge to their targets earlier in training. **(b)** Learning dynamics of individual frequencies over training. **(c)** Training steps required for the Learner to reach a threshold of performance where $q_k(t) > c$, for different cutoff values c. This demonstrates that the learning speed of Fourier modes is slower for higher frequencies.
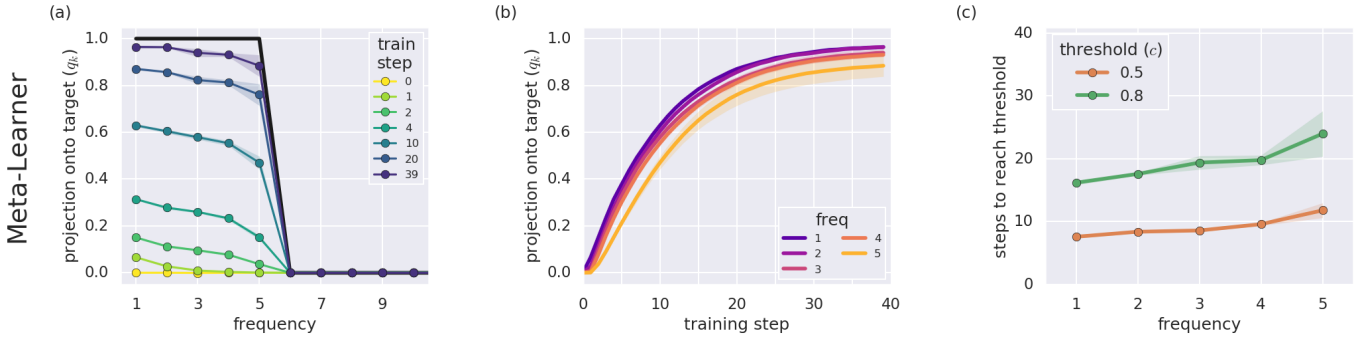
Figure 9. Learning dynamics of the Meta-Learner for different Fourier modes, as in Fig 9.

pattern of learning Fourier modes with lower frequencies faster. Rather, the Meta-Learner learns all (in-distribution) frequencies almost simultaneously, with only a gentle increase in learning time for higher frequencies.

Putting these changes into perspective, the $K = 5^{\text{th}}$ frequency takes the Learner $6.4\times$ as long to learn than the $K = 1$ term, while it causes the Meta-Learner to take only $1.5\times$ as long. [4]

As in the linear regression case, it is instructive to view the difference between the structure that the Learner and Meta-Learner exploit at different milestones of learning. We show this in Fig 10, where it can be clearly seen how the Learner acquires the Fourier structure of nonlinear functions with a staggered time course, while the Meta-Learner acquires all the Fourier structure roughly concurrently.

As in the case of linear regression, this overall difference

---

[4]Indeed, if one accounts for the incomplete learning of the higher frequencies at this point during outer-training, this factor drops to $1.2\times$ (Fig A5).

could not be attributed to differences in parameterisation between the Learner and the Meta-Learner (Fig A6).

4.2.4. RESULTS: OUT-OF-DISTRIBUTION

Finally, we observe that since the Meta-Learner is configured to have an effective prior over Fourier spectra, it suppresses structure outside the support of this distribution.

We outer-trained a Meta-Learner LSTM on bandpass functions, where $a_3 = a_4 = a_5 = 1$, and $a_k = 0 \ \forall k$ otherwise. This Meta-Learner LSTM shows the same learning dynamics on the pass-band as described above, but all stop-band signals are not fit at all (Fig A7). This effect thus appears to be far more dramatic than the bias introduced for linear regression problems, which showed a gradual degradation of learning outside of the training distribution.

4.2.5. RELATIONSHIP TO BAYES-OPTIMAL INFERENCE

As in Section 3.2.6, we again demonstrate that the Meta-Learner shows the same qualitative learning dynamics as can be expected from Bayes-optimal inference on the same
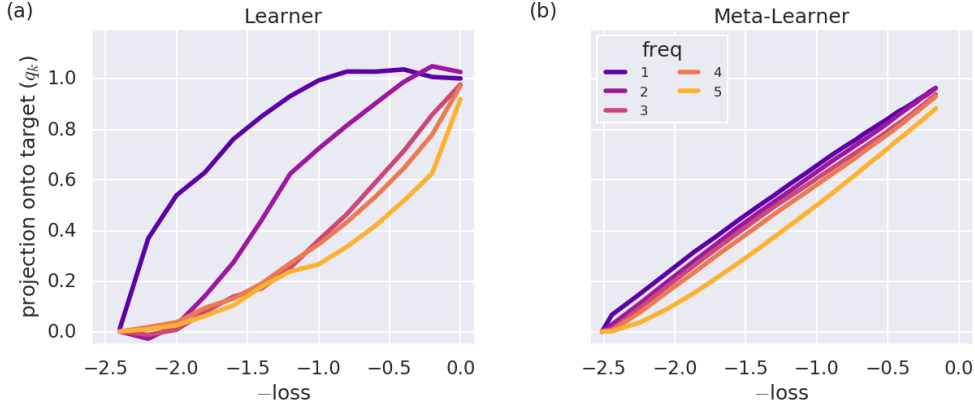
Figure 10. Effective portion of a nonlinear function learned over the course of training, broken down by Fourier components, for **(a)** the Learner, and **(b)** the Meta-Learner, as in Fig 4.

distribution of tasks.

For a simple approximation of Bayes-optimal inference over functions g of the form given in Equation (9), we implemented a tabular look-up table of functions defined in phase space, i.e. where $\phi \in [0, 2\pi]^K$. We subdivided this space into 16 bins along each axis, producing $16^5 \approx 10^6$ functions. We use this to compute a posterior mean function, $\bar{g}_t$, after observing t input-output pairs. In Fig 11, we show the expected projection of the posterior mean function onto the Fourier modes of the ground-truth function. This algorithm learns all Fourier modes concurrently, much like the pattern observed with the Meta-Learner.

4.3. Summary

In this section, we compared how sample-inefficient deep learners, and sample-efficient LSTM Meta-Learners (pre-configured through meta-learning) progressively capture the structure of a nonlinear regression task. While Learners latch on to the Fourier modes in order of their frequency—first the lower frequencies, then the higher ones—the sample-efficient LSTM Meta-Learners estimate all the Fourier modes concurrently. These latter dynamics are congruent with the dynamics of Bayes-optimal inference on the family of nonlinear regression problems on which the Meta-Learners have been trained.

5. Experiment 3: Contextual bandits

In our third experiment, we turn to the dynamics of reinforcement learning. Schaul et al. (2019) describes a phenomenon that occurs during on-policy reinforcement learning: when function approximators are trained on tasks containing multiple contexts, there is an interference effect wherein improved performance in one context suppresses learning for other contexts. This occurs because the data

distribution is under the control of the learner; as a policy for one context is learned, this controls behaviour in other contexts, and prevents the required exploration. This interference does not occur when one learns supervised, or off-policy, or when one trains separate systems for the separate tasks.

Here we first replicate the contextual bandit experiments in Schaul et al. (2019) using a simple Learner (Section 5.1). We then consider the dynamics by which a sample-efficient Meta-Learner—outer-trained to learn contextual bandit problems—acquires structure while learning problems of the same form (Section 5.2). In each case, we compare these learning dynamics to the learning behaviour of decoupled systems, for which the proposed interference should not occur. Analysis of the learning process by which the Meta-Learner itself is constructed is saved for Section 6.

5.1. Learner

5.1.1. SETUP

We consider contextual bandit problems of the following form. We assume that there are K_c contexts (whose identity is fully observed), and K_a actions that are all available in all contexts. Within each context, there is a correct action, which, if taken, delivers a unit reward with probability p_{correct}; if an incorrect action is taken, a unit reward is delivered with probability $p_{\text{incorrect}}$. On each step, the context is sampled randomly.

For our experiments here, we use $K_c = K_a = 5$ contexts and actions. We also use non-deterministic rewards with $p_{\text{correct}} = 0.8$ and $p_{\text{incorrect}} = 0.2$ (though qualitatively identical results were obtained with values of 1 and 0 respectively, as used in Schaul et al. (2019)). We explicitly only consider tasks where the contexts are in conflict with
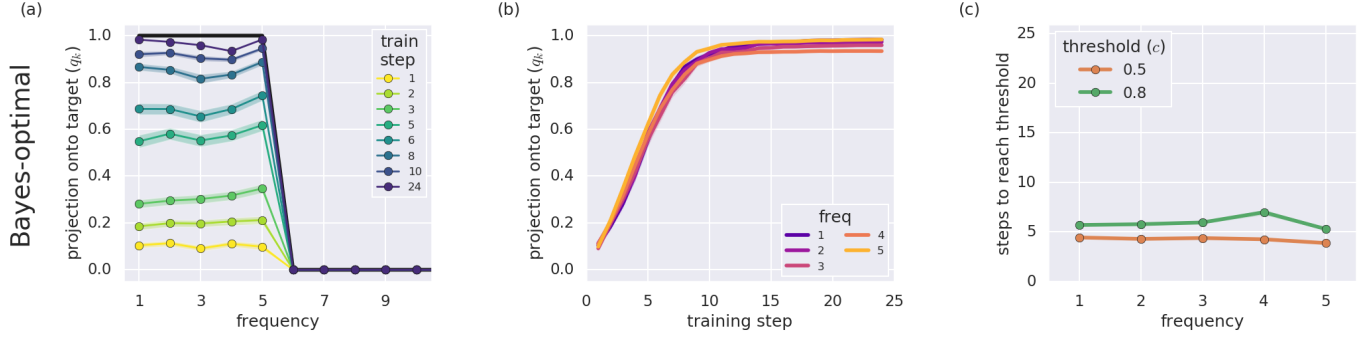
Figure 11. Learning dynamics of Bayesian nonlinear regression for functions g of the form given in Equation (9). Results shown as for Fig 9.

each other, i.e. where each context has a unique correct action.

We use a linear function approximator as our Learner: a simple network that takes the context c as input (represented by a one-hot, $\boldsymbol{c}$), and outputs a policy given by

$$\pi(\boldsymbol{a}|c) = \text{softmax}(\boldsymbol{W}\boldsymbol{c} + \boldsymbol{b}) \quad (11)$$

As described in Schaul et al. (2019), the biases $\boldsymbol{b}$ "couple" the respective contexts' learning processes, causing interference. We train the network via REINFORCE (Williams, 1992) and Adam (see Appendix A.5 for details; similar results obtain using SGD).

We also compare the Learner to one where K_c independent networks handle the policy for each of the K_c contexts. For each network, we use a similar linear + softmax parameterisation as Eqn 11; the cth network is thus effectively tabular, as is the overall policy learned by this system.

5.1.2. HOW TO ASSESS LEARNING DYNAMICS

At each training step, t, we tracked the context-dependent policy $\pi_t(\cdot|c)$, and extracted the probability of taking the correct action in each context, $q_c(t) = \pi_t(a_{\text{correct}}(c)|c)$. This gives the expected reward in context c at time t to be:

$$\mathbb{E}[r_c(t)] = q_c(t)p_{\text{correct}} + (1 - q_c(t))p_{\text{incorrect}} \quad (12)$$

where the (unsubscripted) expectation, $\mathbb{E}$, is over the stochasticity in the policy and the environment. This, in turn, gives the overall expected reward at time t as:

$$\mathbb{E}[r(t)] = \frac{1}{K_c}\sum_c \mathbb{E}[r_c(t)] \quad (13)$$

As our interest was in relating the dynamics of the first-learned context to that of the second-learned context, and the third-, etc, we rank-ordered the contexts by their expected return over the course of training, R_c:

$$R_c = \mathbb{E}_t\mathbb{E}[r_c(t)] \quad (14)$$

Given the linearity of Eqn (12) (and that $p_{\text{correct}} > p_{\text{incorrect}}$), this is equivalent to rank-ordering by the time-average of $q_c(t)$. With this ordering, we switch notation from the cth context to the kth-learned context. Thus, for example, $q_1(t)$ refers to the probability of choosing the correct action at time t for the context that happens to have been learned first.

5.1.3. RESULTS

Fig 12 shows the Learner's learning dynamics for each successively learned context. When learning is coupled across tasks (as in the top row of Fig 12) the Learner takes exponentially longer, on average, to learn each successive context; the 5th context taking on average $\sim 400\times$ as many steps to learn than the 1st context. When tasks are decoupled, so that learning occurs separately for each context (as in the bottom row of Fig 12), the delay between learning each successive context is far more gradual; the 5th context taking on average $\sim 2\times$ as many steps to learn as the 1st context.

5.2. Meta-Learner

5.2.1. SETUP

Does this interference plague all of reinforcement learning? To test this, we sought to compare these learning dynamics with those of a sample-efficient meta-learner, which had been explicitly pre-trained to expect that policies for different contexts are independent of each other.

As in previous Sections, we built an LSTM Meta-Learner that, on every episode during outer-training, was presented with a new sample of a contextual bandits task. In particular, for each length-T episode, i, we sampled a new mapping from contexts to correct actions. Importantly, for each episode, the correct action $a_{\text{correct}}^{(i)}(c)$ for context c was drawn *independently* from the uniform distribution
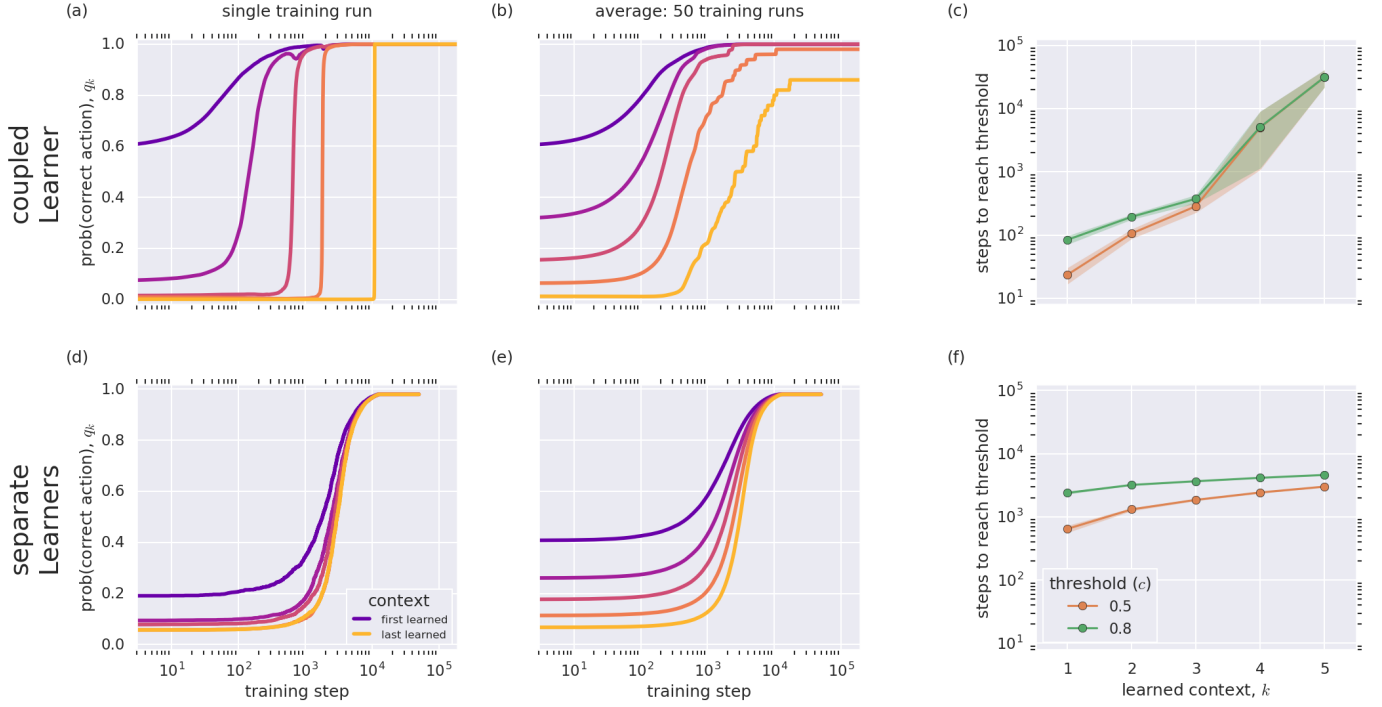
Figure 12. **(a)** Learning dynamics ($q_k(t)$) of the coupled Learner on a single training run. Contexts are ordered by the order in which they are learned. Note the logarithmic time scale on the abscissa. **(b)** As in (a), but averaged over 50 training runs. Data are averaged by the ordered indices, k, rather than the nominal indices, c. **(c)** Training steps required for the Learner to reach a threshold of performance where $q_k(t) > c$, for different cutoff values c. This demonstrates that later-learned contexts take exponentially longer to learn. **(d-f)** As in (a-c), except where separate Learners are used for each context.

over actions. Thus an optimal learner should expect that data gleaned from actions taken in context c are uninformative about a good policy in context c'.

The remainder of the setup was as described in Sections 3.2.1 and 4.2.1, with one notable change: rather than receiving the correct target for the previous time step, $y_{t-1}^{(i)}$, as an input at time t (as is appropriate for supervised meta-learning), we instead feed the Meta-Learner the previous action taken, $a_{t-1}^{(i)}$ and the reward received, $r_{t-1}^{(i)}$, as per Wang et al. (2016). We outer-trained the Meta-Learner with REINFORCE and Adam. We used episode lengths of $T = 100$, and $N_c = N_a = 5$ for consistency with the Learner. Further details are in Appendix A.6.

5.2.2. HOW TO ASSESS LEARNING DYNAMICS

We again consider the inner dynamics here, by which the configured LSTM learns a solution to a new contextual bandits problem. We leave analysis of outer-loop behaviour to Section 6.

Our goal is to estimate the effective policy realised by the LSTM at iteration t of an episode i, which we denote $\pi_t^{(i)}$,

and determine how this policy changes with more observations (i.e., as t increases). In particular, our interest is in the probabilities of taking the correct action in each context, $q_c^{(i)}(t) = \pi_t^{(i)}(a_{\text{correct}}^{(i)}(c)|c)$. We did this in an analogous way to the previous Sections, by forking the LSTM for each time step t during an episode, and probing the forked copies (counterfactually) with all possible contexts.

As with the Learner, we reordered contexts by their expected return over the course of training for that episode, $R_c^{(i)}$, defined analogously to Eqn (14), and we use the index k to refer to the kth-learned context in episode i.

We averaged results over 2000 episodes, and present statistics computed over 15 independently-trained Meta-Learners.

5.2.3. RESULTS

Fig 13 shows the Meta-Learner's learning dynamics for successively-learned contexts, in the same form as Fig 12. We notice again the same discrepancy described in the linear and nonlinear regression cases: while the Learner experiences a profound delay between learning successive contexts (Fig 12), this delay is relatively mild for the Meta-
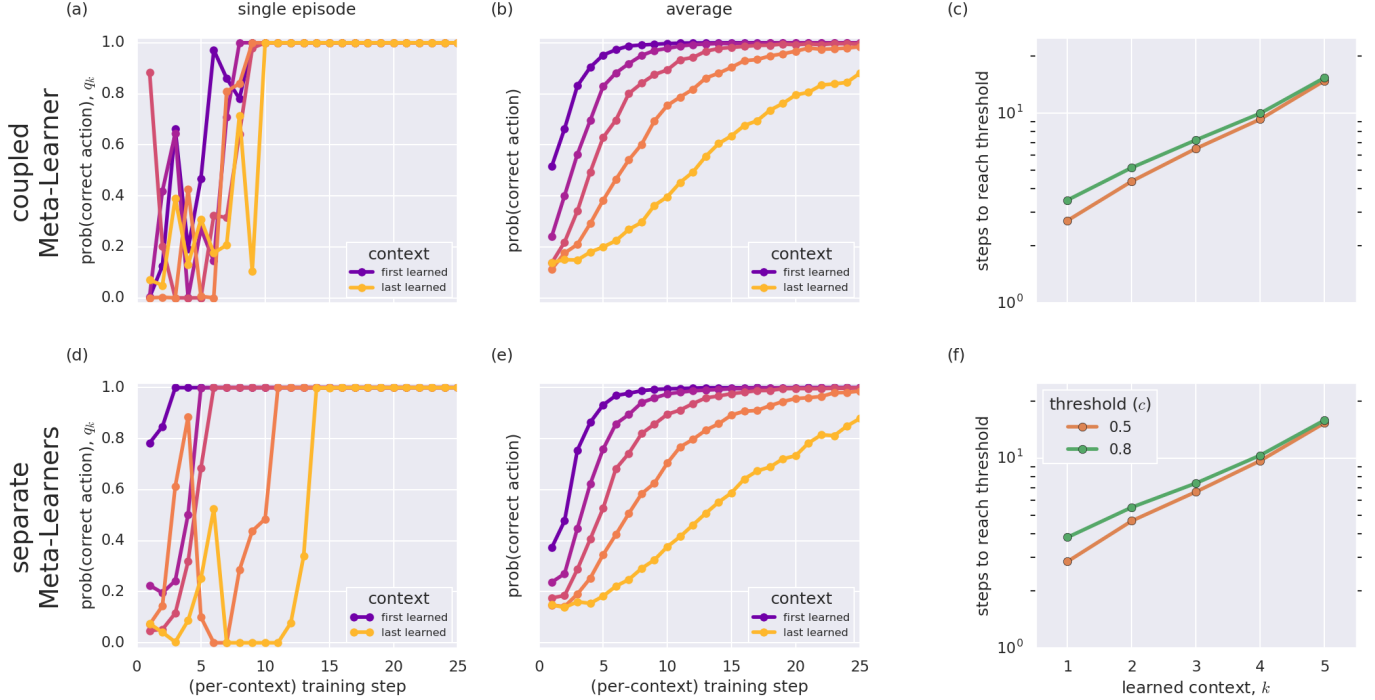
Figure 13. Learning dynamics of the Meta-Learner for successively-learned contexts, as in Fig 12.

Learner (Fig 13). Moreover, there is little difference between these dynamics and the case when the individual learning tasks are decoupled to be learned by separate Meta-Learners: in the coupled case, the 5th context takes on average $4.3\times$ as many steps to learn as the 1st context, compared with $3.9\times$ for the decoupled case. We note that a Bayes-optimal inference algorithm would be expected to show parity between the coupled and separate learning dynamics: as it would have prior knowledge that the contexts in the coupled case are indeed independent, inference over context-specific policies would factorise.

5.3. Summary

In this section, we compared how sample-inefficient reinforcement learners and sample-efficient LSTM Meta-Learners (pre-configured through meta-learning) progressively capture the structure of a contextual bandits task. While Learners experience interference between contexts—wherein learning each context-specific policy interferes with the learning of a policy for other contexts—this interference is not experienced by sample-efficient Meta-Learned LSTMs.

6. Meta-Learners' Outer Loops

The results we have presented so far showcase the behaviour of meta-learned LSTMs *after* significant meta-training had taken place. This analysis was motivated by the desire to compare the learning trajectories taken by a family of sample-efficient learning algorithms with those taken by a family of sample-inefficient learning algorithms.

We now turn to the question: how do these sample-efficient learners themselves get constructed? What trajectories do they take through the space of learning algorithms?

For each of the three experimental setups, we measured how the *inner* learning trajectories progressed at different stages during *outer* learning. These results are shown in Figs 14–16.

Between these results, we note that the patterns of outer learning are not consistent across the three experiments.

In the case of nonlinear regression and contextual bandits, the pattern of outer learning of the Meta-Learner is staggered, thus sharing a resemblance with the learning process of the Learner itself. For nonlinear regression, Fig 15 shows that early in meta-training, the inner learner is able to estimate the low-frequency structure within each task, but it takes many more steps of outer training until the inner learner is capable of estimating the high-frequency struc-

ture. This staggered meta-learning trajectory is analogous to the learning trajectory of the Learner, which acquires the Fourier structure in a similarly ordered fashion (albeit for a single task). This staggered structure is also observed for meta-training on the contextual bandit experiment: Fig 16 shows that there is significant interference between contexts early during meta-training, which is gradually overcome over iterations of the outer loop.

In contrast to these phenomena, the outer learning of the Meta-Learner during linear regression follows an *opposite* pattern. Fig 14 shows that early in meta-training, the inner learner is better able to estimate the lesser singular modes than the greater ones. The ability of the Meta-Learner to estimate singular modes is thus staggered in the opposite direction to that of the Learner, which, early in training, has a better estimate of the greater singular modes than the lesser ones.

Notwithstanding these observations, the learning process of the Learner and the outer learning process of the Meta-Learner are not directly comparable. This is because the task being learned by these respective systems are fundamentally different. For example, in the linear regression problem, the Learner is being configured to solve a single regression problem, while the Meta-Learner, during meta-training, is being configured to be a generic[5] linear regression algorithm. Solutions to these two tasks are radically different from one another; for example, we typically express the optimal solution to a single regression task as a matrix (viz., as the least squares *solution*), while we typically express the optimal solution to generic linear regression via a highly non-linear formula (viz., as the least squares *algorithm*, given in a reduced form in Eqns 6–8). As such, there may be no reason to expect any congruence between the Learners' learning dynamics and the Meta-Learners' outer learning dynamics, or indeed to expect similar outcomes across the three experiments, as the optimal solutions to the respective meta-tasks may look radically different.

7. Discussion

In this work we have shown three convergent pieces of evidence that meta-trained, sample-efficient Meta-Learners pursue systematically different learning trajectories from sample-inefficient Learners when applied to the same tasks.

Our goal here has not been to argue that the meta-learning systems are somehow better than the learners. As is well-known, (meta-trained) meta-learners' sample-efficiency comes at several costs, such as their high degree of task-specificity and the expense of meta-training. These

---

[5](at least, generic on the distribution of regression problems in the meta-training distribution)

are not issues which we attempt to address here. Rather, our goal has been to show that the process by which machine learners acquire a task's structure can differ dramatically once strong priors come into play.

We do not yet know the degree to which the discrepancies we identify between Learners and Meta-Learners extend to other task structures. We chose to focus on these three patterns—staggered learning of singular structure in linear regression, staggered learning of Fourier structure in non-linear regression, and interference between context-specific policies in reinforcement learning—as these have already been described in the existing literature on deep learning and reinforcement learning. There is much to be discovered about how these patterns extend, for example, to the learning of hierarchical or latent structure, or whether they manifest in the learning of rich, complex real-world tasks.

While we have focused on memory-based Meta-Learners, there is additional work to be done to characterise the learning dynamics of other sample-efficient learning systems, including other meta-learning systems. Our expectation is that if these systems behave as if they are performing amortised Bayes-optimal inference with appropriately-calibrated priors, then the learning dynamics should resemble those of the LSTM Meta-Learners we have described here. On the other hand, the learning dynamics may diverge if these models have very strong priors, if they are being pushed to behave out-of-distribution, if they have pronounced capacity limitations, or if they are sufficiently general that their first stage of learning involves producing a complex inference about which task needs to be performed. All of these may hold, for instance, when considering human learners.

We believe that these findings are likely to have implications for curriculum learning. Whether one considers designing curricula for animals (Skinner, 1958; Peterson, 2004), humans (Beauchamp, 1968; Hunkins and Ornstein, 2016; Nation and Macalister, 2009), or machines (Elman, 1993; Sanger, 1994; Krueger and Dayan, 2009; Bengio et al., 2009; Kumar et al., 2010; Lee and Grauman, 2011; Shrivastava et al., 2016; Weinshall and Amir, 2018), the promise of this field is that one can accelerate learning by leveraging information about how the learner learns and how the task is constructed. By putting these together, one can decompose the task into chunks that are more easily learnable for the learner at hand. We have described how different machine learning systems can follow radically different learning trajectories depending on their priors; we may thus need to design radically different curricula for each to accelerate their respective learning.

These ideas may also connect to the challenges of how to bring humans into the loop of machine learning and machine behaviour. Direct human input has been pro-
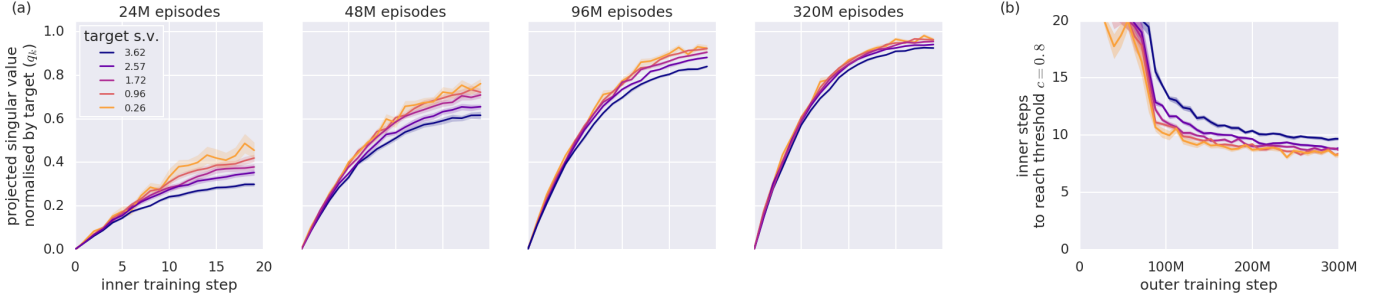
Figure 14. Outer learning dynamics of the Meta-Learner for the linear regression task. **(a)** Inner learning dynamics for linear regression problems at different stages during outer training. Curves shown for the single 5D linear regression task depicted in Fig 4. The final panel shows the qualitative behaviour described in Section 3, whereby the meta-trained Meta-Learner learns all singular modes (roughly) concurrently. **(b)** Steps to reach threshold ($\arg\min t$, s.t. $q_k(t) > 0.8$), as outer training progresses. Note that smaller singular values are learned faster during outer-training.
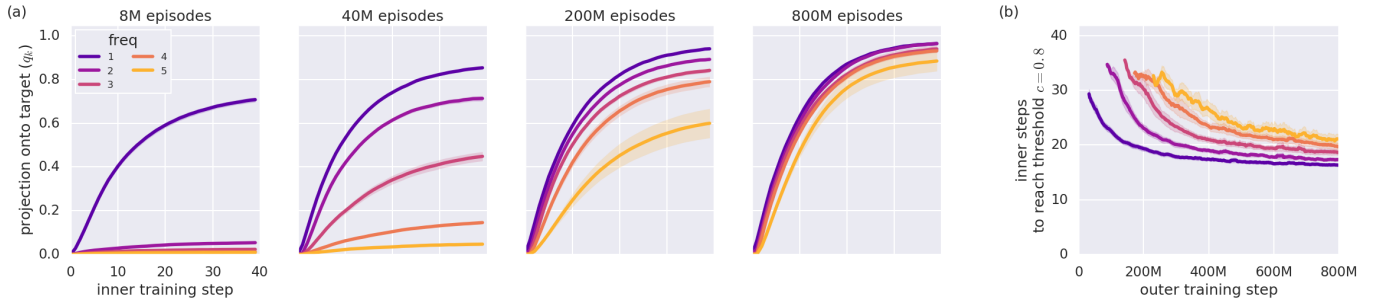

Figure 15. Outer learning dynamics of the Meta-Learner for the nonlinear regression task. Results presented in the same format as Fig 14. The final panel of (a) shows the qualitative behaviour described in Section 4, whereby the meta-trained Meta-Learner learns all Fourier modes (roughly) concurrently. Note the difference in time scale between the outer training of the coupled Meta-Learner and separate Meta-Learners, which shows the presence of interference early in meta-training.

posed both as a means of accelerating machine learning (Ng et al., 1999; Schaal, 1999; Abbeel and Ng, 2004; Wilson et al., 2012; Lin et al., 2017), as well as a way of solving the value-alignment problem (Russell et al., 2015; Amodei et al., 2016; Hadfield-Menell et al., 2016; Bostrom, 2017; Christiano et al., 2017; Fisac et al., 2017; Leike et al., 2018). Either way, this research programme aims to enrich the pedagogical relationship between humans and machines. Successful pedagogy, however, depends on teachers having a rich model of their what their students know and how they learn (Shafto et al., 2014)[6]. Through our work, we have shown that different machine learning systems pursue different learning trajectories; thus, if human teachers expect DL and RL systems to learn like sample-efficient human learners, their teaching strategies are likely to be miscalibrated. This may underlie recent observations made by Ho et al. (2018) that humans provide corrective feedback to virtual RL agents that leads them astray. The

authors' interpretation was that humans' feedback is better described as a communication signal, rather than a reinforcement signal; in our framing, this comes down to a difference between the learning trajectories that different learners are expected to pursue. If we are committed to becoming better teachers, we will need to gain a better understanding of the specific learning trajectories that each of our machine pupils are apt to take.

Acknowledgements

---

[6]and also depends on students having a rich model of teachers' behaviour to infer their communicative intent.
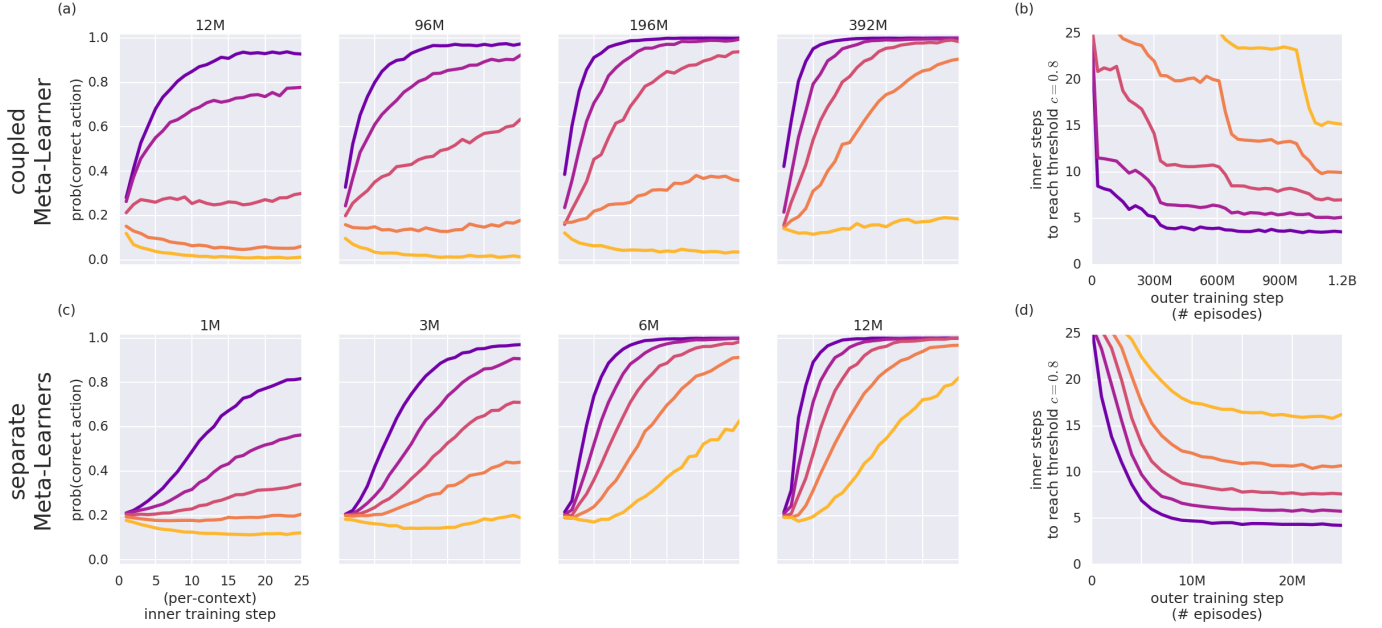
Figure 16. Outer learning dynamics of the Meta-Learner for the bandits regression task. Results presented in the same format as Fig 14. The rightmost panels of (a) and (c) shows the qualitative behaviour described in Setion 5, whereby the meta-trained Meta-Learner learns all contexts without interference, i.e. in a near identical manner across coupled and separate conditions.

Appendices

A. Network architectures

A.1. Linear regression: Learner

For our Learner, we use 2-layer MLPs equipped with SGD; we use no nonlinearities, 10 hidden units, truncated normal initialisation ($\sigma = 0.1$), and learning rate 10^{-3}. All data is procedurally-generated. We train with minibatch size 100. For the 2D problem, we train for 4k minibatches; for the 5D problem, we train for 16k minibatches.

Where we use Adam (Section 3.3), we use an identical setup, with a learning rate of 10^{-3}.

A.2. Linear regression: Meta-Learner

For our Meta-Learner, we use an LSTM equipped with SGD; we use 64 hidden units, and learning rate 10^{-2}. We train with minibatch size 200. We use $T = 20$ steps per episode, and outer-trained over 80M training episodes.

Where we use Adam (Section 3.3), we use a learning rate of 10^{-4}, and outer-trained over 8M training episodes.

A.3. Nonlinear regression: Learner

For our Learner, we use 6-layer MLPs equipped with Adam; we use ReLU nonlinearities, 256 hidden units, and learning rate 10^{-4}. We train with minibatch size 40, and train over 5k minibatches.

A.4. Nonlinear regression: Meta-Learner

For our Meta-Learner, we use an LSTM equipped with Adam; we use 64 hidden units, and learning rate 10^{-4}. We train with minibatch size 200. We use $T = 40$ steps per episode, and outer-trained over 800M episodes.

A.5. Contextual bandits: Learner

For our Learner, we use a linear + softmax network. We initialise the weights with a truncated normal distribution ($\sigma = 1/\sqrt{5}$), including a bias (to induce interference (Schaul et al., 2019)) and train using REINFORCE and the Adam optimiser with learning rate 10^{-4}. We train with minibatch size 200, and train up to when the expected reward, $\mathbb{E}[r(t)]$, reaches 0.98. Similar results were obtained using the SGD optimiser in place of Adam.

A.6. Contextual bandits: Meta-Learner

For our Meta-Learner, we use an LSTM equipped with RE-INFORCE and Adam; we use 64 hidden units, and learn-

ing rate 10^{-4}. We train with minibatch size 200. We use $T = 125$ steps per episode, and outer-trained over 2B episodes.

References

Pieter Abbeel and Andrew Y Ng. Apprenticeship learning via inverse reinforcement learning. In *Proceedings of the twenty-first international conference on Machine learning*, page 1. ACM, 2004.

Alessandro Achille and Stefano Soatto. Emergence of invariance and disentanglement in deep representations. *Journal of Machine Learning Research*, 19(50):1–34, 2018.

Alessandro Achille, Matteo Rovere, and Stefano Soatto. Critical learning periods in deep networks. In *International Conference on Learning Representations*, 2019. URL https://openreview.net/forum?id=BkeStsCcKQ.

Madhu S Advani and Andrew M Saxe. High-dimensional dynamics of generalization error in neural networks. *arXiv preprint arXiv:1710.03667*, 2017.

Ron Amit and Ron Meir. Meta-learning by adjusting priors based on extended pac-bayes theory. In *International Conference on Machine Learning*, pages 205–214, 2018.

Dario Amodei, Chris Olah, Jacob Steinhardt, Paul Christiano, John Schulman, and Dan Mané. Concrete problems in ai safety. *arXiv preprint arXiv:1606.06565*, 2016.

Marcin Andrychowicz, Misha Denil, Sergio Gomez, Matthew W Hoffman, David Pfau, Tom Schaul, Brendan Shillingford, and Nando De Freitas. Learning to learn by gradient descent by gradient descent. In *Advances in Neural Information Processing Systems*, pages 3981–3989, 2016.

Devansh Arpit, Stanisław Jastrzebski, Nicolas Ballas, David Krueger, Emmanuel Bengio, Maxinder S Kanwal, Tegan Maharaj, Asja Fischer, Aaron Courville, Yoshua Bengio, et al. A closer look at memorization in deep networks. *arXiv preprint arXiv:1706.05394*, 2017.

Marco Baity-Jesi, Levent Sagun, Mario Geiger, Stefano Spigler, G Ben Arous, Chiara Cammarota, Yann LeCun, Matthieu Wyart, and Giulio Biroli. Comparing dynamics: Deep neural networks versus glassy systems. *arXiv preprint arXiv:1803.06969*, 2018.

Horace B Barlow. Unsupervised learning. *Neural computation*, 1(3):295–311, 1989.

Jonathan Baxter. Theoretical models of learning to learn. In *Learning to learn*, pages 71–94. Springer, 1998.

Jonathan Baxter. A model of inductive bias learning. *Journal of Artificial Intelligence Research*, 12:149–198, 2000.

George A Beauchamp. Curriculum theory. 1968.

Yoshua Bengio, Jérôme Louradour, Ronan Collobert, and Jason Weston. Curriculum learning. In *Proceedings of the 26th annual international conference on machine learning*, pages 41–48. ACM, 2009.

Alberto Bernacchia, Mate Lengyel, and Guillaume Hennequin. Exact natural gradient in deep linear networks and its application to the nonlinear case. In S. Bengio, H. Wallach, H. Larochelle, K. Grauman, N. Cesa-Bianchi, and R. Garnett, editors, *Advances in Neural Information Processing Systems 31*, pages 5945–5954. Curran Associates, Inc., 2018.

Christopher M. Bishop. *Pattern Recognition and Machine Learning (Information Science and Statistics)*. Springer-Verlag, Berlin, Heidelberg, 2006. ISBN 0387310738.

Nick Bostrom. *Superintelligence*. Dunod, 2017.

Léon Bottou. Large-scale machine learning with stochastic gradient descent. In *Proceedings of COMPSTAT'2010*, pages 177–186. Springer, 2010.

Pratik Chaudhari and Stefano Soatto. Stochastic gradient descent performs variational inference, converges to limit cycles for deep networks. In *2018 Information Theory and Applications Workshop (ITA)*, pages 1–10. IEEE, 2018.

Yutian Chen, Matthew W Hoffman, Sergio Gómez Colmenarejo, Misha Denil, Timothy P Lillicrap, Matt Botvinick, and Nando de Freitas. Learning to learn without gradient descent by gradient descent. In *Proceedings of the 34th International Conference on Machine Learning-Volume 70*, pages 748–756. JMLR. org, 2017.

Anna Choromanska, Mikael Henaff, Michael Mathieu, Gérard Ben Arous, and Yann LeCun. The loss surfaces of multilayer networks. In *Artificial Intelligence and Statistics*, pages 192–204, 2015.

Paul F Christiano, Jan Leike, Tom Brown, Miljan Martic, Shane Legg, and Dario Amodei. Deep reinforcement learning from human preferences. In *Advances in Neural Information Processing Systems*, pages 4299–4307, 2017.

David A Cohn, Zoubin Ghahramani, and Michael I Jordan. Active learning with statistical models. *Journal of artificial intelligence research*, 4:129–145, 1996.
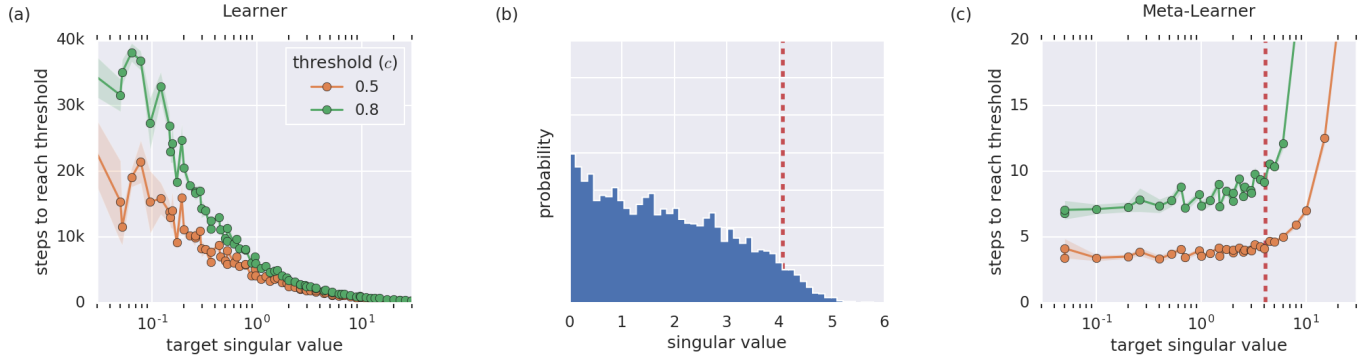
Figure A1. **(a)** Learning dynamics of the Learner for singular modes of different singular values, for 5D matrices (as in Fig 1c). **(b)** Samples from marginal distribution of singular values for 5D matrices from the standard matrix normal distribution (as in Fig 2b.) **(c)** Learning dynamics of the Meta-Learner for singular modes of different singular values, for 5D matrices (as in Fig 3c).
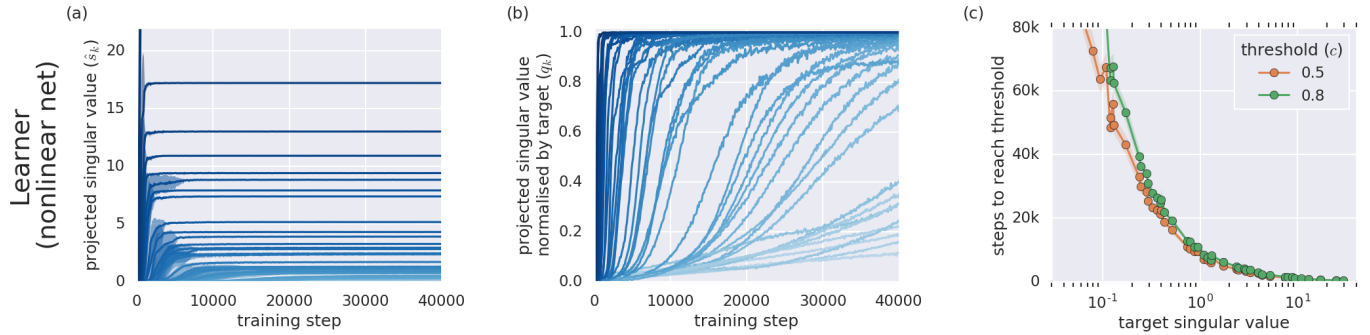

Figure A2. Learning dynamics of a Learner using a nonlinear network, rather than a linear one. We use here a 3-layer MLP, with 10 hidden units per layer, and ReLU nonlinearities (except for the last layer). Results shown for 2D linear regression problems, as in Fig 1.

Francis Crick. The recent excitement about neural networks. *Nature*, 337(6203):129–132, 1989.

Yann N Dauphin, Razvan Pascanu, Caglar Gulcehre, Kyunghyun Cho, Surya Ganguli, and Yoshua Bengio. Identifying and attacking the saddle point problem in high-dimensional non-convex optimization. In *Advances in neural information processing systems*, pages 2933–2941, 2014.

J Michael Davis. Imitation: A review and critique. In *Perspectives in ethology*, pages 43–72. Springer, 1973.

Vikas Dhiman, Shurjo Banerjee, Brent Griffin, Jeffrey M Siskind, and Jason J Corso. A critical investigation of deep reinforcement learning for navigation. *arXiv preprint arXiv:1802.02274*, 2018.

Yan Duan, John Schulman, Xi Chen, Peter L. Bartlett, Ilya Sutskever, and Pieter Abbeel. Rl\$^2\$: Fast reinforcement learning via slow reinforcement learning. *CoRR*, abs/1611.02779, 2016. URL http://arxiv.org/abs/1611.02779.

Jeffrey L Elman. Learning and development in neural networks: The importance of starting small. *Cognition*, 48 (1):71–99, 1993.

SM Ali Eslami, Danilo Jimenez Rezende, Frederic Besse, Fabio Viola, Ari S Morcos, Marta Garnelo, Avraham Ruderman, Andrei A Rusu, Ivo Danihelka, Karol Gregor, et al. Neural scene representation and rendering. *Science*, 360(6394):1204–1210, 2018.

Chrisantha Thomas Fernando, Jakub Sygnowski, Simon Osindero, Jane Wang, Tom Schaul, Denis Teplyashin, Pablo Sprechmann, Alexander Pritzel, and Andrei A Rusu. Meta learning by the baldwin effect. *arXiv preprint arXiv:1806.07917*, 2018.

Chelsea Finn, Pieter Abbeel, and Sergey Levine. Model-agnostic meta-learning for fast adaptation of deep networks. *arXiv preprint arXiv:1703.03400*, 2017.

Jaime F Fisac, Monica A Gates, Jessica B Hamrick, Chang Liu, Dylan Hadfield-Menell, Malayandi Palaniappan,
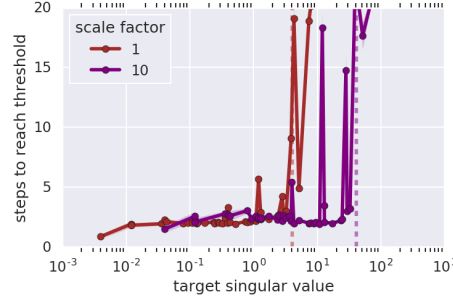
Figure A3. Meta-Learners outer-trained on scaled distributions of singular modes show the same qualitative (inner) learning dynamics, shifted accordingly. Here we show results for Meta-Learners trained with $p(\boldsymbol{W}) = \mathcal{MN}(\boldsymbol{0}, \alpha^2 \boldsymbol{I}, \alpha^2 \boldsymbol{I})$, where the scale factor α is either 1 or 10. Vertical lines show the 95th percentile of the distribution of singular values for each training distribution.
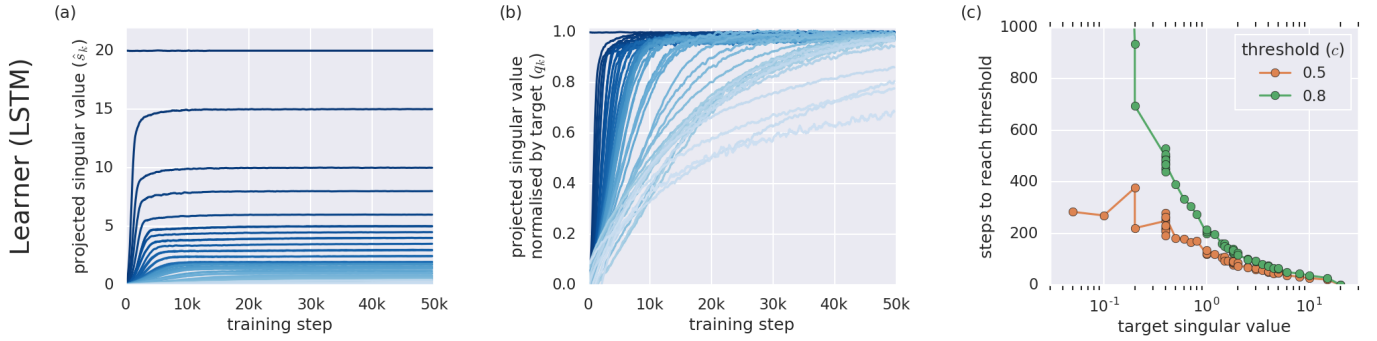

Figure A4. Learning dynamics for a Learner parameterised as an LSTM on 2D linear regression tasks. Results presented as in Fig 1. The setup here was identical to the Meta-Learner (i.e., with precisely the same parameterisation), except instead of sampling a new target matrix $\boldsymbol{W}^{(i)}$ on each episode, the target matrix was kept fixed throughout the whole training process. We show here the behaviour of the learned function at the end of each "episode" (i.e., via the input-output function expressed at the final time step of the LSTM). Nevertheless, the results were qualitatively identical for all "inner" time steps. Despite the congruency between this parameterisation of the Learner, and that of the Meta-Learner, the learning dynamics remain different.

Dhruv Malik, S Shankar Sastry, Thomas L Griffiths, and Anca D Dragan. Pragmatic-pedagogic value alignment. *arXiv preprint arXiv:1707.06354*, 2017.

Meire Fortunato, Mohammad Gheshlaghi Azar, Bilal Piot, Jacob Menick, Ian Osband, Alex Graves, Vlad Mnih, Remi Munos, Demis Hassabis, Olivier Pietquin, et al. Noisy networks for exploration. *arXiv preprint arXiv:1706.10295*, 2017.

Kunihiko Fukushima and Sei Miyake. Neocognitron: A self-organizing neural network model for a mechanism of visual pattern recognition. In *Competition and cooperation in neural nets*, pages 267–285. Springer, 1982.

Bennett G Galef Jr. Imitation in animals: History, definition, and interpretation of data from the psychological laboratory. *Social Learning: Psychological and Biological Perspectives*, page 1, 1988.

Marta Garnelo, Jonathan Schwarz, Dan Rosenbaum, Fabio Viola, Danilo J Rezende, SM Eslami, and Yee Whye Teh. Neural processes. *arXiv preprint arXiv:1807.01622*, 2018.

Christophe Giraud-Carrier, Ricardo Vilalta, and Pavel Brazdil. Introduction to the special issue on meta-learning. *Machine learning*, 54(3):187–193, 2004.

Ian J Goodfellow, Oriol Vinyals, and Andrew M Saxe. Qualitatively characterizing neural network optimization problems. *arXiv preprint arXiv:1412.6544*, 2014.

Erin Grant, Chelsea Finn, Sergey Levine, Trevor Darrell, and Thomas Griffiths. Recasting gradient-based meta-learning as hierarchical bayes. *arXiv preprint arXiv:1801.08930*, 2018.

Umut Güçlü and Marcel AJ van Gerven. Deep neural networks reveal a gradient in the complexity of neural representations across the ventral stream. *Journal of Neuroscience*, 35(27):10005–10014, 2015.
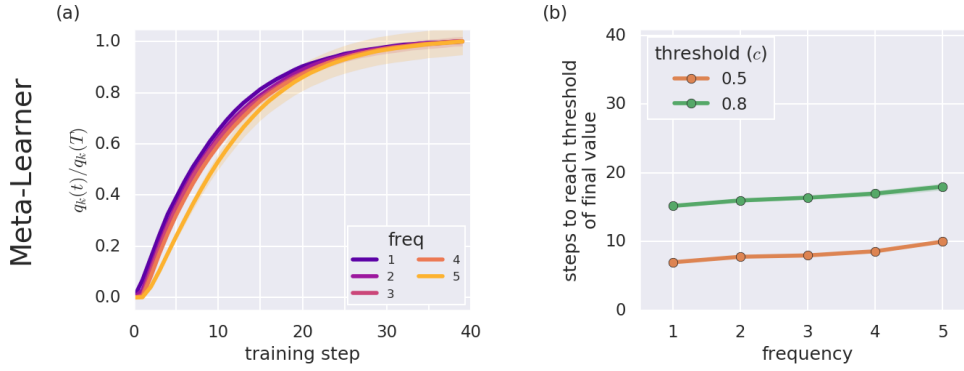
(a) Meta-Learner

(b)

Figure A5. Learning dynamics of the Meta-Learner for different Fourier modes, as in Fig 9. Since we terminated outer-training of the Meta-Learner before convergence (see Section 6), inner learning of higher frequencies did not typically reach the target within the length of the episode. Here we adjust for this by measuring time constants of the curves shown in Fig 9b with respect to their asymptotic value, not with respect to their target value.
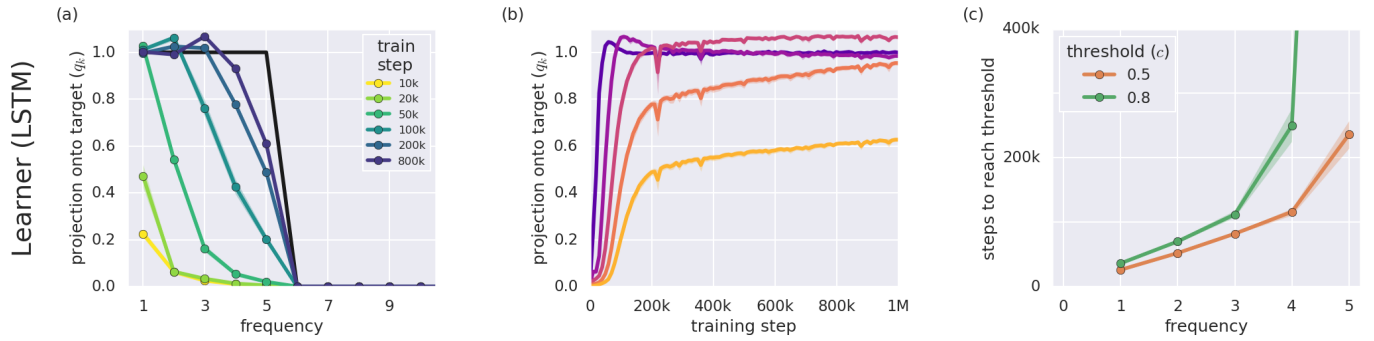

(a) Learner (LSTM)

(b)

(c)

Figure A6. Learning dynamics for a Learner parameterised as an LSTM on nonlinear regression tasks. Results presented as in Fig 8. The setup here mirrored that presented in the control experiment shown in Fig A4, i.e. using an LSTM as with the Meta-Learner, except instead of sampling a new function $g^{(i)}$ on each episode, the function was kept fixed throughout the whole training process. Despite the congruency between this parameterisation of the Learner, and that of the Meta-Learner, the learning dynamics remain different.

Jordan Guerguiev, Timothy P Lillicrap, and Blake A Richards. Towards deep learning with segregated dendrites. *ELife*, 6:e22901, 2017.

Abhishek Gupta, Russell Mendonca, YuXuan Liu, Pieter Abbeel, and Sergey Levine. Meta-reinforcement learning of structured exploration strategies. *arXiv preprint arXiv:1802.07245*, 2018.

Dylan Hadfield-Menell, Stuart J Russell, Pieter Abbeel, and Anca Dragan. Cooperative inverse reinforcement learning. In *Advances in neural information processing systems*, pages 3909–3917, 2016.

James Harrison, Apoorva Sharma, and Marco Pavone. Meta-learning priors for efficient online bayesian regression. *arXiv preprint arXiv:1807.08912*, 2018.

Gillian M Hayes and John Demiris. *A robot controller using learning by imitation*. University of Edinburgh, Department of Artificial Intelligence, 1994.

Donald O Hebb et al. The organization of behavior, 1949.

Takao K Hensch. Critical period regulation. *Annu. Rev. Neurosci.*, 27:549–579, 2004.

Geoffrey E Hinton and Steven J Nowlan. How learning can guide evolution. *Complex systems*, 1(3):495–502, 1987.

Geoffrey E Hinton, Terrence J Sejnowski, et al. Learning and relearning in boltzmann machines. *Parallel distributed processing: Explorations in the microstructure of cognition*, 1:282–317, 1986.

Mark K Ho, Fiery Cushman, Michael L Littman, and Joseph L Austerweil. People teach with rewards and punishments as communication not reinforcements. 2018.

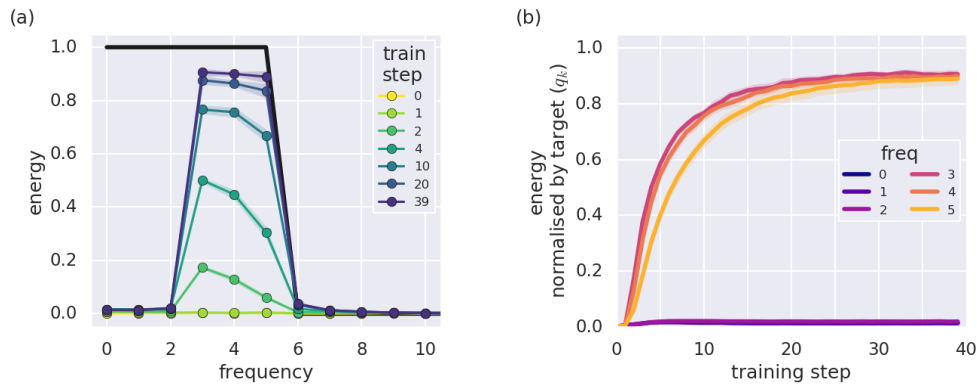Sepp Hochreiter, A Steven Younger, and Peter R Conwell. Learning to learn using gradient descent. In *Interna-*

Figure A7. Learning dynamics of the Meta-Learner for different Fourier modes, when outer-trained to have a pass-band between $K = 3$ and $K = 6$. Results shown here are for nonlinear regression tasks where there is low-pass energy for $K < 3$, but the Meta-Learner does not learn this structure. Panels in the same format as in Fig 3a-b.

tional Conference on Artificial Neural Networks, pages 87–94. Springer, 2001.

Rein Houthooft, Xi Chen, Yan Duan, John Schulman, Filip De Turck, and Pieter Abbeel. Vime: Variational information maximizing exploration. In *Advances in Neural Information Processing Systems*, pages 1109–1117, 2016.

Francis P Hunkins and Allan C Ornstein. *Curriculum: Foundations, principles, and issues*. Pearson Education, 2016.

Thomas Jaksch, Ronald Ortner, and Peter Auer. Near-optimal regret bounds for reinforcement learning. *Journal of Machine Learning Research*, 11(Apr):1563–1600, 2010.

Ingmar Kanitscheider and Ila Fiete. Training recurrent networks to generate hypotheses about how the brain solves hard navigation problems. In *Advances in Neural Information Processing Systems*, pages 4529–4538, 2017.

Seyed-Mahdi Khaligh-Razavi and Nikolaus Kriegeskorte. Deep supervised, but not unsupervised, models may explain it cortical representation. *PLoS computational biology*, 10(11):e1003915, 2014.

Diederik P Kingma and Jimmy Ba. Adam: A method for stochastic optimization. *arXiv preprint arXiv:1412.6980*, 2014.

Kai A Krueger and Peter Dayan. Flexible shaping: How learning in small steps helps. *Cognition*, 110(3):380–394, 2009.

M Pawan Kumar, Benjamin Packer, and Daphne Koller. Self-paced learning for latent variable models. In *Advances in Neural Information Processing Systems*, pages 1189–1197, 2010.

Brenden M Lake, Ruslan Salakhutdinov, and Joshua B Tenenbaum. Human-level concept learning through probabilistic program induction. *Science*, 350(6266): 1332–1338, 2015.

Brenden M Lake, Tomer D Ullman, Joshua B Tenenbaum, and Samuel J Gershman. Building machines that learn and think like people. *Behavioral and Brain Sciences*, 40, 2017.

Andrew K Lampinen and Surya Ganguli. An analytic theory of generalization dynamics and transfer learning in deep linear networks. *arXiv preprint arXiv:1809.10374*, 2018.

Yong Jae Lee and Kristen Grauman. Learning the easy things first: Self-paced visual category discovery. In *Computer Vision and Pattern Recognition (CVPR), 2011 IEEE Conference on*, pages 1721–1728. IEEE, 2011.

Jan Leike, David Krueger, Tom Everitt, Miljan Martic, Vishal Maini, and Shane Legg. Scalable agent alignment via reward modeling: a research direction. *arXiv preprint arXiv:1811.07871*, 2018.

David D Lewis and William A Gale. A sequential algorithm for training text classifiers. In *Proceedings of the 17th annual international ACM SIGIR conference on Research and development in information retrieval*, pages 3–12. Springer-Verlag New York, Inc., 1994.

Hao Li, Zheng Xu, Gavin Taylor, Christoph Studer, and Tom Goldstein. Visualizing the loss landscape of neural nets. In *Advances in Neural Information Processing Systems*, pages 6391–6401, 2018.

Ke Li and Jitendra Malik. Learning to optimize. *arXiv preprint arXiv:1606.01885*, 2016.

Timothy P Lillicrap, Daniel Cownden, Douglas B Tweed, and Colin J Akerman. Random synaptic feedback weights support error backpropagation for deep learning. *Nature communications*, 7:13276, 2016.

Zhiyu Lin, Brent Harrison, Aaron Keech, and Mark O Riedl. Explore, exploit or listen: Combining human feedback and policy model to speed up deep reinforcement learning in 3d worlds. *arXiv preprint arXiv:1709.03969*, 2017.

Adam H Marblestone, Greg Wayne, and Konrad P Kording. Toward an integration of deep learning and neuroscience. *Frontiers in computational neuroscience*, 10:94, 2016.

JL McClelland. A connectionist perspective on knowledge and development. 1995.

Nikhil Mishra, Mostafa Rohaninejad, Xi Chen, and Pieter Abbeel. Meta-learning with temporal convolutions. *CoRR*, abs/1707.03141, 2017. URL http://arxiv.org/abs/1707.03141.

Volodymyr Mnih, Koray Kavukcuoglu, David Silver, Andrei A Rusu, Joel Veness, Marc G Bellemare, Alex Graves, Martin Riedmiller, Andreas K Fidjeland, Georg Ostrovski, et al. Human-level control through deep reinforcement learning. *Nature*, 518(7540):529, 2015.

Ian SP Nation and John Macalister. *Language curriculum design*. Routledge, 2009.

Aran Nayebi, Daniel Bear, Jonas Kubilius, Kohitij Kar, Surya Ganguli, David Sussillo, James J DiCarlo, and Daniel L Yamins. Task-driven convolutional recurrent models of the visual system. In *Advances in Neural Information Processing Systems*, pages 5295–5306, 2018.

Andrew Y Ng, Daishi Harada, and Stuart Russell. Policy invariance under reward transformations: Theory and application to reward shaping. In *ICML*, volume 99, pages 278–287, 1999.

Bruno A Olshausen and David J Field. Emergence of simple-cell receptive field properties by learning a sparse code for natural images. *Nature*, 381(6583):607, 1996.

Ian Osband, Charles Blundell, Alexander Pritzel, and Benjamin Van Roy. Deep exploration via bootstrapped dqn. In *Advances in neural information processing systems*, pages 4026–4034, 2016.

Deepak Pathak, Pulkit Agrawal, Alexei A Efros, and Trevor Darrell. Curiosity-driven exploration by self-supervised prediction. In *International Conference on Machine Learning (ICML)*, volume 2017, 2017.

Jeffrey Pennington, Samuel S Schoenholz, and Surya Ganguli. The emergence of spectral universality in deep networks. *arXiv preprint arXiv:1802.09979*, 2018.

Gail B Peterson. A day of great illumination: Bf skinner's discovery of shaping. *Journal of the Experimental Analysis of Behavior*, 82(3):317–328, 2004.

Jean Piaget. Play, dreams and imitation in childhood. 1952.

Kim Plunkett and Chris Sinha. Connectionism and developmental theory. *British Journal of Developmental Psychology*, 10(3):209–254, 1992.

Lutz Prechelt. Early stopping-but when? In *Neural Networks: Tricks of the trade*, pages 55–69. Springer, 1998.

Neil Rabinowitz, Frank Perbet, Francis Song, Chiyuan Zhang, S. M. Ali Eslami, and Matthew Botvinick. Machine theory of mind. 80:4218–4227, 10–15 Jul 2018. URL http://proceedings.mlr.press/v80/rabinowitz18a.html.

Maithra Raghu, Ben Poole, Jon Kleinberg, Surya Ganguli, and Jascha Sohl Dickstein. On the expressive power of deep neural networks. In *Proceedings of the 34th International Conference on Machine Learning-Volume 70*, pages 2847–2854. JMLR. org, 2017.

Nasim Rahaman, Devansh Arpit, Aristide Baratin, Felix Draxler, Min Lin, Fred A Hamprecht, Yoshua Bengio, and Aaron Courville. On the spectral bias of deep neural networks. *arXiv preprint arXiv:1806.08734*, 2018.

Sachin Ravi and Hugo Larochelle. Optimization as a model for few-shot learning. *ICLR*, 2017.

Larry A Rendell, Raj Sheshu, and David K Tcheng. Layered concept-learning and dynamically variable bias management. In *IJCAI*, pages 308–314, 1987.

Timothy T Rogers and James L McClelland. *Semantic cognition: A parallel distributed processing approach*. MIT press, 2004.

Frank Rosenblatt. The perceptron: a probabilistic model for information storage and organization in the brain. *Psychological review*, 65(6):386, 1958.

Stuart Russell, Daniel Dewey, and Max Tegmark. Research priorities for robust and beneficial artificial intelligence. *Ai Magazine*, 36(4):105–114, 2015.

Andrei A Rusu, Dushyant Rao, Jakub Sygnowski, Oriol Vinyals, Razvan Pascanu, Simon Osindero, and Raia Hadsell. Meta-learning with latent embedding optimization. *arXiv preprint arXiv:1807.05960*, 2018.

Terence D Sanger. Neural network learning control of robot manipulators using gradually increasing task difficulty. *IEEE transactions on Robotics and Automation*, 10(3): 323–333, 1994.

Adam Santoro, Sergey Bartunov, Matthew Botvinick, Daan Wierstra, and Timothy Lillicrap. Meta-learning with memory-augmented neural networks. In *International conference on machine learning*, pages 1842–1850, 2016.

Andrew M Saxe, James L McClelland, and Surya Ganguli. Exact solutions to the nonlinear dynamics of learning in deep linear neural networks. *arXiv preprint arXiv:1312.6120*, 2013.

Andrew M Saxe, James L McClelland, and Surya Ganguli. A mathematical theory of semantic development in deep neural networks. *arXiv preprint arXiv:1810.10531*, 2018a.

Andrew Michael Saxe, Yamini Bansal, Joel Dapello, Madhu Advani, Artemy Kolchinsky, Brendan Daniel Tracey, and David Daniel Cox. On the information bottleneck theory of deep learning. 2018b.

Stefan Schaal. Is imitation learning the route to humanoid robots? *Trends in cognitive sciences*, 3(6):233–242, 1999.

Stefan Schaal, Auke Ijspeert, and Aude Billard. Computational approaches to motor learning by imitation. *Philosophical Transactions of the Royal Society of London B: Biological Sciences*, 358(1431):537–547, 2003.

Roger C Schank. Conceptual dependency: A theory of natural language understanding. *Cognitive psychology*, 3 (4):552–631, 1972.

Tom Schaul, Diana Borsa, Joseph Modayil, and Razvan Pascanu. Ray interference: a source of plateaus in deep reinforcement learning. *arXiv preprint arXiv:1904.11455*, 2019.

Jurgen Schmidhuber, Jieyu Zhao, and Marco Wiering. Simple principles of metalearning. Technical report, SEE, 1996.

Samuel S Schoenholz, Justin Gilmer, Surya Ganguli, and Jascha Sohl-Dickstein. Deep information propagation. *arXiv preprint arXiv:1611.01232*, 2016.

Burr Settles. Active learning. *Synthesis Lectures on Artificial Intelligence and Machine Learning*, 6(1):1–114, 2012.

Patrick Shafto, Noah D Goodman, and Thomas L Griffiths. A rational account of pedagogical reasoning: Teaching by, and learning from, examples. *Cognitive psychology*, 71:55–89, 2014.

Abhinav Shrivastava, Abhinav Gupta, and Ross Girshick. Training region-based object detectors with online hard example mining. In *Proceedings of the IEEE Conference on Computer Vision and Pattern Recognition*, pages 761–769, 2016.

Ravid Shwartz-Ziv and Naftali Tishby. Opening the black box of deep neural networks via information. *arXiv preprint arXiv:1703.00810*, 2017.

Burrhus F Skinner. Reinforcement today. *American Psychologist*, 13(3):94, 1958.

Daniel Soudry, Elad Hoffer, Mor Shpigel Nacson, Suriya Gunasekar, and Nathan Srebro. The implicit bias of gradient descent on separable data. *Journal of Machine Learning Research*, 19(70), 2018.

Christopher H Stock, Alex H Williams, Madhu S Advani, Andrew M Saxe, and Surya Ganguli. Learning dynamics of deep networks admit low-rank tensor descriptions. *ICLR 2018 workshop submission*, 2018.

David G Stork. Is backpropagation biologically plausible. In *International Joint Conference on Neural Networks*, volume 2, pages 241–246. IEEE Washington, DC, 1989.

Weijie Su, Stephen Boyd, and Emmanuel Candes. A differential equation for modeling nesterovs accelerated gradient method: Theory and insights. In *Advances in Neural Information Processing Systems*, pages 2510–2518, 2014.

Richard S Sutton and Andrew G Barto. Reinforcement learning: An introduction. 1998.

Haoran Tang, Rein Houthooft, Davis Foote, Adam Stooke, OpenAI Xi Chen, Yan Duan, John Schulman, Filip DeTurck, and Pieter Abbeel. # exploration: A study of count-based exploration for deep reinforcement learning. In *Advances in Neural Information Processing Systems*, pages 2753–2762, 2017.

Edward L Thorndike. Animal intelligence. 1911.

Sebastian Thrun. Lifelong learning algorithms. In *Learning to learn*, pages 181–209. Springer, 1998.

Sebastian Thrun and Lorien Pratt. Learning to learn: Introduction and overview. In *Learning to learn*, pages 3–17. Springer, 1998.

Mariya Toneva, Alessandro Sordoni, Remi Tachet des Combes, Adam Trischler, Yoshua Bengio, and Geoffrey J Gordon. An empirical study of example forgetting during deep neural network learning. *arXiv preprint arXiv:1812.05159*, 2018.

Alan M Turing. Computing machinery and intelligence. *Mind*, 49:433–460, 1950.

Oriol Vinyals, Charles Blundell, Tim Lillicrap, Daan Wierstra, et al. Matching networks for one shot learning. In *Advances in Neural Information Processing Systems*, pages 3630–3638, 2016.

Jane X Wang, Zeb Kurth-Nelson, Dhruva Tirumala, Hubert Soyer, Joel Z Leibo, Remi Munos, Charles Blundell, Dharshan Kumaran, and Matt Botvinick. Learning to reinforcement learn. *arXiv preprint arXiv:1611.05763*, 2016.

Daphna Weinshall and Dan Amir. Theory of curriculum learning, with convex loss functions. *arXiv preprint arXiv:1812.03472*, 2018.

Andre Wibisono, Ashia C Wilson, and Michael I Jordan. A variational perspective on accelerated methods in optimization. *Proceedings of the National Academy of Sciences*, 113(47):E7351–E7358, 2016.

Ronald J Williams. Simple statistical gradient-following algorithms for connectionist reinforcement learning. *Machine learning*, 8(3-4):229–256, 1992.

Aaron Wilson, Alan Fern, and Prasad Tadepalli. A bayesian approach for policy learning from trajectory preference queries. In *Advances in neural information processing systems*, pages 1133–1141, 2012.

Zhi-Qin J Xu, Yaoyu Zhang, and Yanyang Xiao. Training behavior of deep neural network in frequency domain. *arXiv preprint arXiv:1807.01251*, 2018.

Zhiqin John Xu. Understanding training and generalization in deep learning by fourier analysis. *arXiv preprint arXiv:1808.04295*, 2018.

Daniel LK Yamins, Ha Hong, Charles F Cadieu, Ethan A Solomon, Darren Seibert, and James J DiCarlo. Performance-optimized hierarchical models predict neural responses in higher visual cortex. *Proceedings of the National Academy of Sciences*, 111(23):8619–8624, 2014.

Lin Yang, Raman Arora, Tuo Zhao, et al. The physical systems behind optimization algorithms. In *Advances in Neural Information Processing Systems*, pages 4377–4386, 2018.